



Deposited via The University of Leeds.

White Rose Research Online URL for this paper:

<https://eprints.whiterose.ac.uk/id/eprint/98957/>

Version: Accepted Version

---

**Article:**

Gomis-Cartesio, LE, Poyatos-More, M, Flint, SS et al. (2017) Anatomy of a mixed-influence shelf edge delta, Karoo Basin, South Africa. Geological Society Special Publications, 444 (1). pp. 393-418. ISSN: 0305-8719

<https://doi.org/10.1144/SP444.5>

---

(c) 2016, The Author(s). Published by The Geological Society of London. All rights reserved. This is an author produced version of a paper published in Geological Society Special Publications. Uploaded in accordance with the publisher's self-archiving policy. Link to published version: <http://doi.org/10.1144/SP444.5>

**Reuse**

Items deposited in White Rose Research Online are protected by copyright, with all rights reserved unless indicated otherwise. They may be downloaded and/or printed for private study, or other acts as permitted by national copyright laws. The publisher or other rights holders may allow further reproduction and re-use of the full text version. This is indicated by the licence information on the White Rose Research Online record for the item.

**Takedown**

If you consider content in White Rose Research Online to be in breach of UK law, please notify us by emailing [eprints@whiterose.ac.uk](mailto:eprints@whiterose.ac.uk) including the URL of the record and the reason for the withdrawal request.

1           **Anatomy of a mixed-influence shelf-edge delta, Karoo Basin, South Africa**

2  
3           LUZ E. GOMIS-CARTESIO<sup>1</sup>, MIQUEL POYATOS-MORÉ<sup>1</sup>, STEPHEN S. FLINT<sup>1</sup>, DAVID M.  
4           HODGSON<sup>2</sup>, RUFUS L. BRUNT<sup>1</sup> & AND HENRY DE V. WICKENS<sup>3</sup>

5           <sup>1</sup>*Stratigraphy Group, School of Earth, Atmospheric and Environmental Sciences, University of*  
6           *Manchester, Manchester M13 9PL, UK.*

7           <sup>2</sup>*Stratigraphy Group, School of Earth and Environment, University of Leeds, Leeds LS2 9JT, UK.*

8           <sup>3</sup>*Geo-Routes Petroleum, 37 Zevendal Road, Kuils River 7580, South Africa.*

9  
10   **Abstract:** The position and process regime of paralic systems relative to the shelf-edge rollover is a  
11   major control on sediment transfer into deep water. The depositional strike and dip variability of an  
12   exhumed Permian shelf-edge succession has been studied in the Paardeberg Ridge, Karoo Basin.  
13   Siltstone-rich slope turbidites are overlain by 25-75 m-thick prodelta parasequences. These are  
14   truncated by a 30 m-thick sandstone-prone unit of tabular or convex-topped sandstones, interpreted  
15   as wave-modified mouth bars, cut by multiple irregular concave-upward erosive surfaces overlain by  
16   sandstones, interpreted as distributary channels. The stratigraphic context, lithofacies, and  
17   architecture are consistent with a mixed-influence shelf-edge delta, and the erosional base to the unit  
18   marks a basinward shift in facies, consistent with a sequence boundary. Channels become thicker,  
19   wider, more erosive, and incise into deeper water facies down dip and correlate to sandstone-rich  
20   upper-slope turbidites, all of which support bypass of sand across the rollover. The overall  
21   progradational stacking pattern results in a stratigraphic decrease in channel dimensions. Results of  
22   this study suggest a predictable relationship between channel geometry, facies and position on the  
23   shelf-to-slope profile under a mixed wave and fluvial process regime.

24  
25   **Keywords:** *shelf edge, rollover, distributary channel, reworked mouth bars, Karoo Basin*

26  
27  
28   Basin margin progradation and the timing of sediment transport to the oceans is strongly influenced  
29   by the position and character of paralic systems relative to the physiography of the shelf-edge rollover  
30   (e.g. Edwards 1981; Mayall *et al.* 1992; Sydow & Roberts 1994; Morton & Suter 1996; Steel *et al.*

31 2000; Muto & Steel 2002; Porębski & Steel 2003; Steel *et al.* 2003; Saller *et al.* 2004; Carvajal & Steel  
32 2009; Covault *et al.* 2009; Dixon *et al.* 2012a). The presence of gullies and channels, which incise into  
33 shelf-edge deltas and act as conduits for sediment transport, have been widely described and  
34 associated with multiple factors, including lowering of relative sea level, headward erosion of  
35 submarine canyons, gravitational instabilities and slope failure, gravity flows and/or high fluvial  
36 discharge, among others (e.g. Pratson *et al.* 1994; Fulthorpe *et al.* 1999, 2000; Muto & Steel 2002;  
37 Plink-Björklund & Steel 2002; Donovan 2003; Porębski & Steel 2003; Posamentier & Kolla 2003;  
38 Petter & Steel 2005; Plink-Björklund & Steel 2005; Jackson & Johnson 2009; Sanchez *et al.* 2012b;  
39 Sylvester *et al.* 2012; Prélat *et al.* 2015).

40 In contrast to reflection seismic data, exhumed shelf-margins provide the resolution needed to  
41 constrain the interplay of sedimentary processes responsible for channel and gully initiation at the  
42 shelf-edge rollover (Hubbard *et al.* 2010). Typically, however, shelf-edge deltas are interpreted to be  
43 dominated by a particular process regime (Dixon *et al.* 2012b). Mixed-influenced systems are rarely  
44 reported (Mellere *et al.* 2003; Pontén & Plink-Björklund 2009; Bowman & Johnson 2014), and the fine-  
45 scale down dip changes in channel geometry and infill architecture across the shelf-edge rollover  
46 have not been documented at outcrop. Most published examples of exhumed rollovers are from high-  
47 gradient shelf margins with short slope lengths (Pyles & Slatt 2000; Mellere *et al.* 2002; Plink-  
48 Björklund & Steel 2005; Carvajal & Steel 2006; Pyles & Slatt 2007; Pontén & Plink-Björklund 2009;  
49 Helland-Hansen 2010). This contrasts with the generally low gradients observed in many seismic  
50 datasets (e.g. Pirmez *et al.* 1998; Cattaneo *et al.* 2007; Patruno *et al.* 2015) that are challenging to  
51 constrain at outcrop (e.g. Dixon *et al.* 2012a; 2012b; Jones *et al.* 2013).

52 The importance of lateral variability in shelf margin physiography, and distribution of erosional and  
53 depositional process regimes, is highlighted in modern (e.g. Olariu & Steel 2009) and three-  
54 dimensional reflection seismic datasets (e.g. Suter & Berryhill 1985; Matteucci & Hine 1987; Poag *et al.*  
55 *et al.* 1990; Tesson *et al.* 1990; Milton & Dyce 1995; Fulthorpe & Austin 1998; Kolla *et al.* 2000; Saller *et al.*  
56 *et al.* 2004; Hadler-Jacobsen *et al.* 2005; Crumeyrolle *et al.* 2007; Ryan *et al.* 2009; Henriksen *et al.*  
57 2011; Moscardelli *et al.* 2012; Sanchez *et al.* 2012a, b; Bourget *et al.* 2014). Outcrop studies focus on  
58 determining clinoform and rollover geometries down depositional-dip profiles (e.g. Steel *et al.* 2000;  
59 Plink-Björklund & Steel 2002; Mellere *et al.* 2003; Plink-Björklund & Steel 2005; Pyles & Slatt 2007;

60 Uroza & Steel 2008; Dixon *et al.* 2012a). Documented outcrop examples with large-scale along-strike  
61 control are rare (e.g. Dixon *et al.* 2012a; Jones *et al.* 2015).

62 In this study, a rare example of an exhumed paralic succession in a shelf-edge rollover position with  
63 extensive depositional-strike and dip constraints is presented from the Permian Waterford Formation  
64 in the Tanqua depocentre, Karoo Basin, South Africa. The outcrops permit the following objectives to  
65 be addressed: i) to describe the vertical transition from slope to shelf deposits and to identify the  
66 shelf-edge rollover and ii) to discuss the origin, evolution and infill of channel-form features across the  
67 slope to shelf transition.

68

### 69 **Geological setting**

70 The Late Carboniferous-Triassic Karoo Basin (Fig. 1) has been interpreted as a retroarc foreland  
71 basin with subsidence caused by flexural loading by the Cape Fold Belt (Johnson 1991; Cole 1992;  
72 Visser 1993; Veevers *et al.* 1994; Catuneanu *et al.* 1998). However, more recent studies have  
73 suggested that subsidence was due to long wavelength dynamic topography effects driven by the  
74 subducting palaeo-Pacific plate (Tankard *et al.* 2009). The fill of the Karoo Basin comprises the 5+ km  
75 thick Karoo Supergroup (Smith 1990) (Fig. 2a). Glacial deposits of the late Carboniferous Dwyka  
76 Group are overlain by Ecca Group post-glacial strata of the Prince Albert, Whitehill, and Collingham  
77 formations, which show a deepening trend from shallow water carbonates to basin plain turbidites (De  
78 Beer 1992; Turner 1999; Johnson *et al.* 2006). In the Tanqua Depocentre, the Collingham Formation  
79 is overlain by ~800 m of mudstones of the Tierberg Formation (Fig. 2a). Overlying these mudstones,  
80 the Skoorsteenberg Formation comprises sandstone-rich basin-floor fans 1-4 (Bouma & Wickens  
81 1991; Wickens 1994; Scott *et al.* 2000; Johnson *et al.* 2001; Andersson *et al.* 2004; Hodgson *et al.*  
82 2006), overlain by a channelised slope wedge of Unit 5 (Wild *et al.* 2005). These deposits are topped  
83 by slope to shelf sediments of the Kookfontein and Waterford formations (Wickens 1994; Wild *et al.*  
84 2009; Oliveira *et al.* 2011; Dixon *et al.* 2012a; 2012b, here all referred to as the Waterford Fm.), which  
85 are the focus of this study (Fig. 2).

86

### 87 **Dataset and methods**

88 The Waterford Formation crops out across the north-eastern part of the Tanqua depocentre, providing  
89 a study area of up to ~1600 km<sup>2</sup>. This study is focused on the Paardeberg Ridge locality (Fig. 1b),

90 which exposes the stratigraphic transition from slope to shelf deposits (Fig. 2b) over an area of up to  
91 10 km<sup>2</sup>. The outcrop (Fig. 1c) is a 150 to 400 m-high, 5 km-long NW-SE trending ridge with a steep  
92 SW face and gullied NE face that provides good three-dimensional control (Fig. 1c). The overall  
93 tabular and laterally continuous succession has been informally divided into lower, middle and upper  
94 units (Fig. 2b and 3). The 30-40 m thick sandstone-rich middle unit displays a complex assemblage of  
95 tabular or convex-topped sandstones cut by irregular concave-upward erosive surfaces overlain by  
96 sandstones, and is the main focus of this study.

97 Four regional (1:50 scale) sedimentary logs (DRs, DR1, DR6 and OUS) provide the general  
98 stratigraphic context and are combined with 10 detailed logs (1:25 scale), focused on the middle unit,  
99 to characterise the different erosional and depositional features in each locality (1090 m of cumulative  
100 logged thickness). Physical correlation of stratigraphic units was constrained by walking out key  
101 surfaces between logs, on both faces of the ridge and in intervening areas to map and capture  
102 depositional dip and strike changes in facies and geometries. All observations were recorded on high-  
103 resolution photo-panels, satellite imagery and aerial photographs (Fig. 1c and 3). Palaeocurrent  
104 measurements (n=670) were taken from planar and trough cross-bedding foresets, ripple-cross  
105 lamination, primary current lineation, basal tool marks and channel-margin orientations (Fig. 4). A  
106 stratigraphic hierarchy based on lithofacies, palaeocurrent measurements and key surfaces was  
107 developed to capture the stacking patterns across multiple scales and to understand the temporal  
108 changes in erosion and deposition.

109

## 110 **Facies analysis**

111 Lithofacies have been defined based on lithology, grain size, and sedimentary structures in Table 1  
112 and are interpreted in terms of depositional processes. Facies associations are described using  
113 lateral and vertical relationships, and interpreted in terms of different depositional environments.

114

### 115 *Lithofacies*

116 A primary classification is based on three main facies groups, according to the maximum grain size  
117 observed within single beds (Table 1 and Fig. 5): conglomerate (C); sandstone (S) and mudstone  
118 (M); the latter includes the spectrum of grain populations from coarse silt to clay.

119

120 *Facies associations*

121 FA-1: Diffuse laminated to structureless mudstones. Dark grey to green fissile to blocky mudstone  
122 bed sets. Commonly structureless fine-medium siltstone (*Md, Mo*), interbedded with coarse-siltstone  
123 beds (*Ms*) with occasional parallel lamination, isolated/starved mm-scale ripples or gently undulating  
124 lamination. Bioturbation is low to moderate.

125 These facies are interpreted to represent deposition from suspension fallout, although some of their  
126 coarser and laminated components indicate deposition from dilute turbidity currents (Macquaker &  
127 Bohacs 2007; Schieber *et al.* 2007). The depositional environment is interpreted to record offshore  
128 deposition below storm wave base on the outer shelf or upper slope (Wild *et al.* 2009; Jones *et al.*  
129 2013). This facies association forms the bulk of the strata in the lower part of the regional succession  
130 (lower unit).

131

132 FA-2i: Heterolithic siltstone-prone thin beds. Thin- to very thin-bedded (cm- to mm-scale) planar and  
133 current-ripple cross-laminated siltstone (*Ms*), interbedded with minor amounts of ripple-laminated  
134 (unidirectional or bidirectional) very fine-grained sandstones (*Sr, Sw*), which commonly show inverse-  
135 to normal-graded composite beds (*Sg*). These deposits can form laterally extensive tabular packages  
136 (several hundred metres) or wedges of slightly inclined strata (a few tens of metres) that drape and/or  
137 onlap erosion surfaces. Bioturbation is low to moderate, and the presence of organic debris is  
138 common.

139 This facies association is interpreted to record either deposition from low-concentration turbulent  
140 suspension flows that developed distally or laterally from denser hyperpycnal flows (Plink-Björklund &  
141 Steel 2004; Bhattacharya & MacEachern 2009; Zavala *et al.* 2011), or deposition from dilute turbidity  
142 currents in unconfined settings. This facies association has been interpreted to reflect deposition in a  
143 distal prodelta/offshore transition environment relatively far from the sediment feeder system, but still  
144 recording the effects of waves.

145

146 FA-2ii: Heterolithic sandstone-prone thin beds. Laterally-extensive (up to several hundreds of metres)  
147 1 to 15 m-thick packages of thin-bedded (cm-scale) parallel or ripple-laminated, inverse or normal  
148 graded, very-fine grained sandstone (*Sl, Sr, Sw*) alternating with planar- and current ripple-laminated  
149 siltstone (*Ms*). Locally, erosional bed bases and inverse grading are observed in thin sandstone beds,

150 and ripple-lamination includes asymmetrical, combined or symmetrical forms. In places, this facies  
151 association includes medium- to thick-beds (up to 50 cm) of partially amalgamated, fine-grained  
152 sandstone (*Ss, Sg, Sl*) forming lenticular packages. Bioturbation is moderate to high, and the  
153 presence of unclassified organic fragments is common.

154 This facies association is interpreted to record the deposits of moderate- to low-concentration turbidity  
155 currents in both confined (within erosive surfaces) and unconfined settings (tabular and laterally  
156 extensive packages). Commonly, the association passes laterally into silt-prone heterolithic deposits  
157 (*FA-2i*), and suggests deposition in a proximal prodelta/shoreface-offshore transition setting  
158 (Hampson 2000; Hampson & Howell 2005). The local thicker sandstone beds reflect deposition from  
159 rapidly expanding, energetic turbulent suspension flows. This facies association can also be found in  
160 marginal or upper parts of channelised elements (Fig. 3b and 6).

161

162 *FA-3i: Thin- to medium-bedded sandstones.* Laterally-persistent parallel-sided, fine-grained  
163 sandstone bedsets intercalated with thinner very-fine grained sandstone bedsets. Beds are up to 20  
164 cm-thick. Some beds are normally or inversely graded (*Sg*), without structures, but most of them show  
165 a range of sedimentary structures including parallel lamination (*Sp*, Fig. 5e), trough cross-bedding or  
166 low angle or hummocky cross-stratification (*Sx, Sl*, Fig. 5e-f), and bed tops exhibit both symmetrical  
167 and asymmetrical ripple forms (*Sr, Sw*, Fig. 5g-h). Climbing-ripple cross-lamination is common.  
168 Bioturbation is generally from moderate to high, and organic fragments are commonly observed in  
169 bedding planes.

170 Normal and/or inverse graded beds are interpreted to represent deposition from river-derived waning  
171 and/or waxing sediment-laden flows, respectively (e.g. Mulder *et al.* 2003; Plink-Björklund & Steel  
172 2004; Petter & Steel 2006; Olariu *et al.* 2010). The structured beds indicate tractional reworking by  
173 high concentration flows and, in the case of climbing ripples, high sedimentation rates possibly  
174 associated with abrupt decrease in flow confinement.

175 The depositional environment of *FA-3i* is interpreted depending on the dominance of particular  
176 sedimentary structures. The planar, trough and climbing ripple cross-lamination facies association is  
177 related to deposition from unidirectional flows in distal mouth bars. Where low-angle, HCS-swaley  
178 cross-stratification in cleaner sandstones predominates, deposition is interpreted to be in a distal  
179 wave-influenced delta front or lower shoreface setting (e.g. Hampson 2000; Bhattacharya & Giosan

180 2003; Hampson & Howell 2005). Thin-bedded sandstones are also observed in marginal or upper  
181 parts of channelised bodies (Fig. 3b & 6).

182

183 FA-3ii: Medium- to thick-bedded sandstones. Laterally extensive or channelised, very fine- to fine-  
184 grained, predominantly structureless or graded sandstone (*Ss*, *Sg*, Fig. 5c-d) bedsets, contain  
185 amalgamation surfaces, scattered mudstone clasts (*Cm*, Fig. 5b), and fluid-escape structures.  
186 Structureless divisions can pass upward into thick-bedded parallel laminated (*Sp*, Fig. 5e) or very low  
187 angle cross-laminated sandstones (*Sl*), which in turn pass upward into asymmetrical or symmetrical  
188 ripple-laminated thick-bedded sandstones. Laterally, bedsets either onlap directly onto inclined  
189 erosional surfaces or pass laterally into thin-bedded sandstones (*FA-3i*) or interbedded sandstones  
190 and siltstones (*FA-2*). In channelised examples, the lower part of this facies association usually  
191 includes intraformational pebble-size mudstone clasts in irregular horizons of clast-supported  
192 conglomerate to sandy matrix-supported conglomerate in a sandy matrix (*Ci*). Bioturbation is highly  
193 variable, from low to high, and organic fragments in bedding planes can be present.

194 The nature of the structureless or graded sandstone beds suggests rapid deposition and frictional  
195 freezing from high-density sediment gravity flows with a high fallout rate that prevents bedload  
196 transport and traction in the base of the flow (e.g. Mutti *et al.* 2003; Tinterri 2007). Basal mudstone  
197 clast horizons are residual lag deposits of material eroded and left behind by largely bypassing flows  
198 (Stevenson *et al.* 2015). Parallel laminated beds could be associated with upper-flow-regime plane  
199 bedding or downstream migration of very low-amplitude long-wavelength bedforms, as has been  
200 described in younger fluvial deposits of the Beaufort Group (Turner 1981; Stear 1983; Stear 1985;  
201 Wilson *et al.* 2014). Cross- and ripple-laminated beds indicate aggradation and traction processes.  
202 This facies association suggests relatively high-energy depositional environments and is found either  
203 filling central parts of concave-up erosion surfaces (scour- or channel-fills), or in the upper part of  
204 lenticular/tabular elements interpreted as mixed-influenced proximal mouth bars (Fig. 3b and 6).

205

206 FA-4: Deformed facies associations. Laterally discontinuous packages of folded and distorted sandy  
207 or silty thin- (*FA-1, 2*) to thick-beds (*FA-3*) that can extend laterally for several hundred metres. They  
208 show a wide spectrum of soft-sediment deformation types, ranging from complete destruction of  
209 primary sedimentary structures and contorted sandstone clasts floating in a sandy/silty matrix, to units

210 with coherent upward directed folds in sandstones. They usually contain large-scale (<5 m-high) fluid-  
211 escape structures and commonly occur associated with erosional and irregular surfaces.

212 Depending on the original structures and relative stratigraphic position, deformation is interpreted to  
213 record a spectrum of processes, from *in-situ* foundering to remobilisation (Owen 2003; Wild 2005;  
214 Wild *et al.* 2009; Oliveira *et al.* 2011; Jones *et al.* 2013), related to failure or gravitational collapse in  
215 oversteepened delta front or channel margin settings. These deposits represent approximately 30% of  
216 the middle unit and are also present in the lower part of the upper unit (Fig. 2b, 3b and 6).

217

### 218 **Stratigraphic evolution**

219 The lower Waterford Formation in the study area is informally divided into lower, middle, and upper  
220 units (Figs.2 and 3). The lower unit succession starts with a 30-40 m-thick dark grey mudstone (FA-1),  
221 with some isolated sandstone bedsets up to 3 m-thick (FA-3ii). This is overlain by four 20 to 75 m-  
222 thick heterolithic coarsening- and thickening-upward packages (FA-1 to FA-2ii), each starting with a  
223 regionally extensive mudstone (FA-1). The succession is abruptly overlain by the 30 m thick middle  
224 unit, which comprises tabular or convex-topped deformed sandstones incised by multiple erosive  
225 surfaces overlain by sandstones (FA-2 and FA-3). The middle unit is capped by a 2 m thick regionally  
226 extensive mudstone (Fig. 3b), above which the upper unit comprises thinner (10-50 m) sandier and  
227 deformed coarsening- and thickening-upward packages with progressively lower mudstone content.  
228 These packages are overlain by a mudstone-dominated unit, with relatively isolated sandstone beds  
229 or bedsets that are either tabular or channelised (FA-3i and FA3-ii). A gradual change in colour from  
230 dark grey to green and purple is observed in the uppermost mudstones.

231 The basal mudstone-prone lower unit with intercalated sandstone beds is interpreted as slope  
232 mudstones and turbidites. The overlying four coarsening- and thickening-upward heterolithic  
233 packages of the lower unit are interpreted as dominated by prodelta and offshore deposits. The  
234 vertical profile and the scale of these stratigraphic packages are consistent with parasequences  
235 bounded by flooding surfaces as described by Van Wagoner *et al.* (1990), and their stratigraphic  
236 setting is consistent with an upper slope position. This parasequence set is overlain abruptly by  
237 erosional channel-fills and deformed lobate bodies (mixed-influence mouth bars) of the middle unit,  
238 described and interpreted in detail below. The regional capping mudstone is interpreted as containing  
239 a flooding surface. The sandier, thinner and deformed deposits of the upper unit are interpreted as

240 wave-dominated or mixed-influenced shelf delta/shoreface parasequences (Wf of Ainsworth *et al.*  
241 2011). These are overlain by isolated fluvial sandstone bodies within grey-green and purple floodplain  
242 mudstones of the lower Beaufort Group (Wilson *et al.* 2014).

243

#### 244 *Palaeocurrent analysis and palaeoshoreline orientation*

245 Palaeocurrent analysis in this study, combined with previous publications on the Waterford Fm. and  
246 underlying submarine fan systems in the Tanqua depocentre, indicate a uniform regional palaeoflow  
247 to the NE and N, with a slope and overlying shelf oriented approximately NW-SE (Johnson *et al.*  
248 2001; van der Werff & Johnson 2003; Wild *et al.* 2005; Hodgson *et al.* 2006; Luthi *et al.* 2006; Wild *et al.*  
249 2009; Jones *et al.* 2013). In the mud-prone lower unit (*FA-1*), there is a general E-to-NE  
250 unidirectional palaeoflow, with an E-W trend from symmetrical ripples in sandstone beds (Fig. 4a).  
251 The overlying parasequences show a N-to-NE spread in unidirectional current ripples and a NE-SW  
252 trend for the bidirectional indicators (Fig. 4a). All this evidence suggests that the NW-SE orientation of  
253 the Paardeberg Ridge outcrop is a strike section to the palaeoshoreline and shelf-edge during  
254 progradation of the basin margin (Fig. 7).

255

#### 256 **Depositional elements in the middle unit**

257 Architectural descriptions of the Paardeberg Ridge exposure (Fig. 3) are focused on the sandstone-  
258 dominated middle unit, which is characterised by two geometries: channelised and lobate.

259

#### 260 *Channelised bodies*

261 In cross-section (Fig. 3), these bodies have basal concave-up surfaces (Fig. 6) that truncate  
262 underlying deposits with up to 20 m of incision. Individual channel bodies (Table in Fig.6) range from  
263 5 to 20 m-thick and 50 to 400 m-wide which, given the strike orientation of the outcrop, are close to  
264 true widths. They can be followed, in planform view (Fig. 7), for up to 350 m down dip where they  
265 increase in width and thickness downdip. Commonly, they are cut by younger erosion surfaces, so  
266 that only remnant fills are preserved (Fig. 6). Where fully preserved, cross-sectional geometries range  
267 from symmetric (Fig. 6) to asymmetric with one steeper erosive side and the other side showing a low  
268 angle contact and a lateral facies change (Fig. 3b and 6). Loaded or slightly deformed bases and  
269 abundant mudstone-clast conglomerates close to erosional bases are common (Fig. 3b and 6).

270 Facies associations within channelised bodies stack to form fining- and thinning-upward packages  
271 (Fig. 8), which in most cases also fine and thin laterally (Fig. 6). Packages have basal mudstone-clast  
272 conglomerates (Fig. 5a-b) overlain by thick-bedded structureless sandstones (*FA-3ii*, Fig. 5c) that  
273 grade vertically and laterally into parallel-laminated (Fig. 5e) or very low angle laminated thick-bedded  
274 sandstones (*FA-3i*). These deposits pass gradually upward into thin-bedded sandstones (<30 cm;  
275 *FA-3i*), which in turn may grade vertically and laterally into interbedded sandstones (up to 15 cm-  
276 thick) and siltstones (*FA-2ii* and *FA-2i*), with a gradual decrease in sandstone content (Fig. 6 and 8).  
277 Sandstones in the thin-bedded and interbedded packages are either structureless, parallel-laminated  
278 or with symmetrical and asymmetrical ripple cross lamination and commonly show symmetrical  
279 rippled tops.

280 These bodies are interpreted to be channel deposits, showing multiple phases of cut and fill. Their  
281 facies associations and position are consistent with subaqueous distributary channels in a deltaic  
282 setting but, their scale, localisation and the processes responsible for their origin and fill are discussed  
283 below.

284

#### 285 *Lobate bodies*

286 These bodies are generally lens-shaped in cross-section with irregular bases (deformed or slightly  
287 erosive) and flat to convex-up tops, although cross-sectional geometry can be modified by  
288 subsequent channel erosion (Fig. 3 and 6). Axes comprise fine-grained sandstone thinning laterally  
289 into finer grained facies. Lobate bodies (Table in Fig.6) range from 5 to 10 m-thick and from 75 to 600  
290 m-wide (true width) and have been mapped for up to 300 m down dip (Fig. 7). Typically, they overlie  
291 thinner, off-axis parts of older lenticular bodies (Fig. 6) or previously deposited channelised elements  
292 (Fig. 6), indicating a compensational stacking pattern (Fig. 3b).

293 Facies associations in lobate bodies stack in coarsening- and thickening-up packages (approx. 15m-  
294 thick) (Fig. 6 and 8). Commonly, a lower section of sand-prone interbedded siltstones and sandstones  
295 (*FA-2ii*) coarsens upwards into thin-bedded sandstone (*FA-3i*). Sandstone beds are normally graded  
296 with parallel lamination and both asymmetrical and symmetrical ripple lamination. Most bed tops show  
297 symmetrical ripples. Towards the upper part of the bodies soft-sediment deformed packages (*FA-4*;  
298 Fig. 8) show slightly erosive, heavily distorted or loaded bases (Fig. 6). Where primary fabric is  
299 preserved, in most cases it is thick-bedded sandstone (*FA-3ii*) and/or interbedded sandstone and

300 siltstone (*FA-2i* and *FA-2ii*). Flames and other fluid escape structures at loaded bed bases can reach  
301 up to 4 m-high. Thin to thick-bedded sandstones with abundant climbing ripple lamination (*FA-3*, Fig.  
302 5f) are commonly found above, below or between deformed deposits, sometimes eroding the  
303 underlying deformed deposits, or in blocks within the deformed packages.

304 The mixed process origin with indicators of both river- and wave-regime, and widespread soft-  
305 sediment deformation in these lenticular sandstone bodies makes them challenging to assign a  
306 simple interpretation. However, the modified coarsening-upward trends with unidirectional currents,  
307 with reworked bed tops, and the close association with subaqueous distributary channels, leads us to  
308 interpret and refer to them as mixed-influence (wave and river) and remobilised mouth bars that were  
309 reworked into more strike elongate lobate geometries.

310

### 311 **Architecture and stratigraphic evolution of the middle unit**

312 Cross-cutting relationships between sedimentary bodies allow reconstruction of the relative ages of  
313 the channelised and lobate deposits ( $tx_C$  or  $tx_L$  respectively in Fig. 3) and therefore the stratigraphic  
314 evolution of the middle unit to be interpreted.

315 The architecture suggests a spatial relationship between the underlying deposits and the positioning  
316 of younger elements. Superposition of channels and mixed-influence mouth bars follows a complex  
317 temporal distribution (Fig. 3), consistent with lateral compensation processes. Combined with the  
318 facies associations, the architecture could also indicate the proximity to an input point at this locality  
319 (Olariu & Bhattacharya 2006; Olariu & Steel 2009).

320 In general, the older channelised elements are sandier, with more structureless sandstone, and wider  
321 (Fig. 3b and 6) than the younger channels. Commonly, they cut into deeper water offshore facies and  
322 also locally into prodelta and/or deformed mixed-influence mouth bars (Fig. 3b). Most of these older  
323 channels show multiple scours with abundant mudstone clast lags (Fig. 3b and 6), which may suggest  
324 recurrent erosion processes and sediment bypass at the same location over time. Younger channels  
325 display a wider spectrum of facies associations, and are generally narrower with simpler cuts (Fig. 6).  
326 Cleaner basal surfaces, less amalgamation, and considerably less mudstone clast lags at their bases  
327 are consistent with less erosive and shorter-lived channels. Typically, these younger channels cut  
328 shallower water facies associations (deformed mixed-influence mouth bars) and their fills show a

329 greater degree of wave reworking towards their tops, suggesting deposition in a shallower water  
330 setting.

331

### 332 *Lateral and vertical relationships between depositional elements*

333 Typically, a lobate element (or mixed-influence mouth bar) is cut or partially eroded by a channelised  
334 element (Fig. 6 and 8). The basal incision surfaces of channelised bodies usually cut from the top of  
335 the underlying lobate element. The presence of collapsed mixed-influence mouth bar facies in  
336 channel-fills has been locally observed (Fig. 8 and 9) indicating that channels were open conduits and  
337 suggesting a close relationship between mouth bar deposition and channel forming processes (Olariu  
338 & Bhattacharya 2006). Channelised bodies are in turn overlain by younger lobate elements, and this  
339 pattern is repeated vertically and laterally along the outcrop.

340

### 341 *Palaeocurrents in the middle unit*

342 In channelised bodies, unidirectional measurements from current and climbing ripples, low angle  
343 cross bedding, and basal groove marks show a dominant NE and N trend, with a dispersion of up to  
344 90° (Fig. 4a & b). Orientation of channel margins support the general SW to NE trend (Fig. 7). Current  
345 ripple lamination from channel margin thin beds show a NE trend, and symmetrical ripples are  
346 oriented NE-SW (Fig. 4b), consistent with the regional wave reworking measurements (Fig. 4a).  
347 Palaeocurrents in the mixed-influence mouth bars or lobate elements show a similar bidirectionality  
348 (NE-N to SW-S) but the unidirectional measurements show a dominant northward trend with a spread  
349 of 90° (Fig. 4c). Orientations from the upper parts of mixed-influence mouth bars or lobate elements  
350 show a wider spread than the lower parts (Fig. 4c). The consistent unidirectional NE trends, and the  
351 dominant, consistent NE-SW (040°-220° to 080°-260°) trend of bidirectional measurements from  
352 symmetrical ripple crest lines (Fig. 4d) supports the overall NW-SE shoreline orientation.

353

## 354 **Discussion**

### 355 *A mixed-influence shelf-edge delta*

356 The Paardeberg Ridge locality lies 15 km down dip of, and approximately 200 m stratigraphically  
357 above the well documented Tanqua deepwater succession, which comprises basin floor fans 1-4  
358 (Wickens 1994; Hodgson *et al.* 2006) and the Unit 5 lower slope turbidite succession (Wild *et al.*

359 2005). This regional framework provides an upper slope stratigraphic context for the lower unit of the  
360 Paardeberg Ridge (mudstones and 20-75 m thick parasequences dominated by thin bedded  
361 heterolithics). The thinner (10-25 m), sandier parasequences of the upper unit, with common  
362 occurrence of HCS and symmetrical ripples, are interpreted as wave dominated and mixed-influenced  
363 shelf parasequences and share many characteristics with the Waterford Formation in other parts of  
364 the basin-fill (Wild *et al.* 2009; Jones *et al.* 2013, 2015). The sandstone-rich middle unit, which  
365 separates the underlying upper slope from overlying shelf deposits, marks an abrupt increase in the  
366 amount of erosion and soft-sediment deformation, with proximal facies associations of sandstone-rich  
367 mixed-influence mouth bars (*FA-3*) cut by sandstone-rich distributary channel-fills (*FA-2* and *FA-3*).  
368 The stratigraphic context, combined with facies analysis and palaeocurrent data, supports the  
369 interpretation of the middle unit as a shelf-edge deltaic package that formed during progradation  
370 towards the NE. The Karoo palaeo-shelf margin is generally considered as a low gradient (Wild *et al.*  
371 2009), stable slope type (*sensu* Ross *et al.* 1994), with limited syn-sedimentary growth faulting  
372 (Jones *et al.* 2013), and widespread amount of soft-sediment deformation and localised slumps (Wild  
373 *et al.* 2009; Oliveira *et al.* 2011; Jones *et al.* 2013).

374 The fill of channelised elements in the middle unit commonly comprises thick-bedded structureless  
375 axial sandstones that pass laterally through thin-bedded sandstones to interbedded channel margin  
376 sandstones and siltstones (Fig. 6 and 8). Bed tops with symmetrical ripples following the regional NE-  
377 SW palaeocurrent trend are found in the thin-bedded channel margin and uppermost parts of the  
378 channel fills. While large storm waves can rework the sea floor at water depths greater than 100 m  
379 the ubiquity of symmetrical ripples and consistency of palaeocurrents indicate deposition above fair  
380 weather wave base during channel filling. The thickness and generally structureless character in axial  
381 to marginal thick-bedded deposits suggest high-energy conditions, but dune-scale bedforms in  
382 channelised elements are rare. This paucity of cross-bedding can be attributed either to unusually  
383 high discharges during short, temporary flash-flood events (Stear 1983) or to the inhibition of bedform  
384 formation due to the narrow grain size range (clay to fine sand) in the whole Karoo Basin (Southard  
385 1971; Turner 1981; Van den Berg & Van Gelder 1993), which constrains the spectrum of possible  
386 sedimentary structures to lower and upper phase plane bedding, and ripples (Rubin & McCulloch  
387 1980; Southard & Boguchwal 1990). Low-angle cross-stratification is locally observed, and has been  
388 associated with very low-amplitude unidirectional bed forms (e.g. Turner 1981; Stear 1983; 1985;

389 Wilson *et al.* 2014), but also to combined-flow structures such as hummocky cross-stratification  
390 (Nøttvedt & Kreisa 1987; Southard *et al.* 1990). However, its expression is difficult to recognize and  
391 interpret in the absence of a wider grain size range. The facies and architectural elements of the  
392 studied succession suggests that different process regimes coexisted at the same location during  
393 clinothem progradation, and as such is a rare example of an exhumed mixed-influence shelf-edge  
394 system. Mixed-influence shelf-edges have been observed in modern systems (e.g. Ainsworth *et al.*  
395 2011; Olariu 2014), and in a few studies of ancient shelf margins (e.g. Olariu *et al.* 2012; Sanchez *et*  
396 *al.* 2012b; Jones *et al.* 2015).

397

#### 398 *Relative sea level at the shelf edge*

399 Parasequences of the lower unit show an overall progradational trend (DRs in Fig. 1b and DR1, DR6  
400 and OUS in Fig. 10). The highly tabular character (Fig. 3a) and absence of lateral compensational  
401 stacking are interpreted to record relatively high accommodation conditions on the upper slope-lower  
402 unit (Wild *et al.* 2009). The sharp and erosional basal contact of the sand-rich middle unit, with its  
403 mixed-influence mouth bar and distributary channels directly truncating upper slope thin beds (Fig. 1b,  
404 3b and 10), indicates a basinward shift of the facies belt. Highly erosive elements and evidence of  
405 sediment instability, the multi-storey stacking and limited thickness (approx. 30 m; Fig. 3b) of the  
406 middle unit are consistent with an abrupt change into a more proximal facies succession in a lower  
407 accommodation setting.

408 The abrupt change in depositional environments and stacking patterns in the middle unit does not  
409 support a simple progradational trend, which would display a gradual upward increase in sandstone  
410 content of parasequences as the delta approached the shelf edge. The basal erosion surface (t1<sub>c</sub>;  
411 Fig. 3b) of the middle unit is therefore interpreted as a sequence boundary (*sensu* Posamentier *et al.*  
412 1988), juxtaposing a paralic succession onto the shelf edge rollover as a response to a relative fall in  
413 sea level. No palaeosol deposits, roots or desiccation cracks have been found to indicate subaerial  
414 exposure of the shelf edge, which suggests that shelf edge accommodation was reduced but  
415 remained subaqueous. A similar situation has been documented in the Laingsburg depocentre by  
416 Jones *et al.* (2013), who interpreted this absence of subaerial exposure as consistent with a Type 2  
417 sequence boundary (*sensu* Posamentier *et al.* 1988). Correlation of the middle unit 1-3 km down dip  
418 to the Ouberg Pass area (Fig. 10) has revealed a succession of sandstone-dominated turbidites,

419 which are interpreted to represent significant sediment bypass through the shelf edge rollover  
420 channels. The flooding surface overlying the middle unit (Fig. 3b) marks a relative rise in sea level.  
421 Sufficient new accommodation was subsequently generated on the shelf to allow deposition of shelf  
422 parasequences of the upper unit, which are thinner, sandier and display shallower facies associations  
423 than those of the lower unit (Fig. 1b and 3a).

424

#### 425 *Shelf-edge channel geometry and initiation mechanisms*

426 Additional evidence of a shelf-edge rollover setting is derived from mapping (Fig. 7) and correlation  
427 between the two sides of the Paardeberg Ridge, which provides a planform control (100 to 350 m dip  
428 section) for the channelised elements of the middle unit (Figs. 7 and 9). Channels are thicker, more  
429 incised, with a greater amount of mudstone clast lags and soft sediment deformation on the down dip  
430 north-eastern side of the ridge than on the up dip south-western side (Fig. 9). On the up dip side of  
431 the ridge, channels cut deformed mixed-influence mouth bar deposits (Figs. 3b and 9) or older  
432 channel fills while on the down dip side they also cut down into prodelta and offshore deposits. This  
433 basinward increase in channel dimensions and depth of erosion is interpreted to reflect the increased  
434 gradient and accommodation across the shelf-edge. The steeper gradient enhances the depth of  
435 erosion of distributary channels (Olariu & Bhattacharya 2006; Jackson & Johnson 2009), and the  
436 onset of gravity driven density flows and gravitational collapse of channel margins across the rollover  
437 (e.g. Bowman & Johnson 2014) (Figs. 10 and 11). Residual deposits, amalgamation surfaces and  
438 multi-storey stacking in the channels of the middle unit suggest relatively long-lived sediment bypass.  
439 This is consistent with the existence of a gullied/scoured slope. Two kilometres farther down dip (NE  
440 of the Paardeberg ridge; Figs. 1c and 10) the prodelta-offshore succession is abruptly overlain by  
441 thick-bedded (0.5-1m thick) normally graded sandstones that pass from structureless to climbing  
442 ripple cross laminated. The beds are lens shaped with erosional bases and sole marks oriented NE-  
443 SW (parallel to the main palaeocurrent direction). These deposits are interpreted as turbidites, and  
444 the basinward upper slope expression of the middle unit (Figs. 10 and 11).

445 Although erosional features and sediment conduits (channels and gullies) are commonly observed at  
446 the shelf edge rollover (e.g. Porębski & Steel 2003; Sylvester *et al.* 2012; Bowman & Johnson 2014;  
447 Prélat *et al.* 2015), the processes involved in their origin require a wide range of possibilities to be  
448 considered. Several mechanisms of subaqueous scouring on the outer shelf region are rejected due

449 to the scale and orientation of the incisions or the latitude of the basin at that time (between 40-60°  
450 degrees south, Faure & Cole 1999). These include glacial scouring or bottom currents from melting  
451 (e.g. Ridente *et al.* 2007), longshore currents (e.g. Lewis 1982; Galloway 1998; Mazières *et al.* 2013),  
452 shallow-water bottom currents (e.g. Viana *et al.* 2002), and density cascades (e.g. Wilson & Roberts  
453 1995; Shapiro & Hill 1997; Ivanov *et al.* 2004). Erosion from tide- or storm-generated rip currents or  
454 surges has been also invoked as a cause for the inception and maintenance of shelf-edge conduits  
455 (Lewis 1982; Huthnance 1995; Clifton 2006; Normandeau *et al.* 2014), and hyperpycnal flows, wave-  
456 supported gravity flows or inertial currents can keep conduits open (Huthnance 1995). These  
457 mechanisms cannot be discarded as they can develop local defects that potentially evolve into larger  
458 channels as the delta progrades and increases sediment supply, leading to loading and  
459 destabilisation of the area (Lewis 1982).

460 Steeper slopes at the shelf-edge rollover, combined with relatively high sediment loads associated  
461 with mouth bar progradation, create conditions for soft-sediment deformation to occur (Owen 2003;  
462 Oliveira *et al.* 2011). The amount of soft-sediment deformation (30%), combined with the observed  
463 interaction between channels and mixed-influence mouth bar deposits in the middle unit (Fig. 3b)  
464 suggest a close association between channel formation and delta-related instabilities (Oliveira *et al.*  
465 2011). Channel incisions are apparently randomly located, but sometimes overlie the axial location of  
466 the underlying mixed-influence mouth bar. The local gradient change around the shelf-edge rollover,  
467 combined with localised high sediment influx and loading (Wild *et al.* 2009) could have created  
468 unstable points around axial positions of mixed-influence mouth bars. Liquefaction and deformation,  
469 particularly in their central and thicker parts, were highly susceptible to local remobilisation and  
470 gravitational collapse (e.g. Jackson & Johnson 2009), creating discrete bathymetric lows that may  
471 have evolved into long-lived conduits through the bypass of gravity flows, generating a highly erosive  
472 and channelised shelf-edge rollover.

473

#### 474 *Accretion and progradation of a shelf-edge rollover*

475 The deformed and sandier parts of lobate elements are generally 5 to 10 m-thick and 80 to 600 m-  
476 wide, whereas channels are 5 to 20 m-thick and 50 to 300 m-wide (Fig. 3b and 6). These geometrical  
477 proportions are not typical of terminal distributary systems (e.g. Olariu & Bhattacharya 2006; Olariu *et*  
478 *al.* 2010) since delta-related deposits would be expected to be significantly thicker compared to the

479 documented channel dimensions. In the Cretaceous Blackhawk Formation of the Book Cliffs (Utah),  
480 prodeltaic channels formed by river-derived hyperpycnal flows are just a few metres thick and  
481 encased within mudstone (Pattison 2005; Pattison *et al.* 2007).

482 In shelf-confined mixed fluvial- and wave-influenced delta systems, feeder channels decrease in size  
483 as they reach the lower delta plain, where distributaries split, avulse and decrease in dimensions as  
484 they become terminal (Bhattacharya & Giosan 2003; Bhattacharya 2006). Observations made in dip  
485 and strike sections at both sides of the Paardeberg Ridge outcrop suggest that when distributary  
486 channels reached the shelf-edge rollover, enhanced erosive and bypass processes created larger  
487 incisions, and channels became larger and deeper moving downslope across the shelf edge rollover  
488 (Figs. 9 and 10). The significant gradient change across the shelf edge rollover may also explain the  
489 abrupt facies changes seen in the dip direction. This process might be particularly enhanced when  
490 associated with relative sea level fall (Talling 1998; Muto & Steel 2002; Porębski & Steel 2006) and  
491 with the proximity of a feeder system (e.g. Mellere *et al.* 2003; Olariu & Bhattacharya 2006). The  
492 cross-cutting relationships between channel elements and lobate bodies suggest that the sudden loss  
493 of confinement led to deposition of mixed-influence mouth bars that forced distributary channels to  
494 step laterally. The smaller channel size up section could reflect the start of backstepping as gradient  
495 decreased when approaching the flooding surface above. However, considering that channels are  
496 larger and erode more deeply basinward (NE; Fig. 10), the up-section reduction in size within the  
497 middle unit is proposed to characterise progradation across the shelf edge rollover (Fig. 11).

498

## 499 **Conclusions**

500 The Paardeberg Ridge locality allows the spatial and temporal evolution of a NE prograding shelf  
501 margin to be constrained in depositional dip and strike sections. Palaeocurrent data indicate a NW-SE  
502 oriented shoreline with dominant NE-SW wave reworking. Truncation of a shallowing upward  
503 succession from upper slope turbidites to shelf edge deposits by a 30 m-thick sandstone-rich unit of  
504 deformed and mixed-influence mouth bars and subaqueous distributary channels represents an  
505 abrupt juxtaposition of paralic deposits on to the shelf edge rollover. The basal erosion surface of the  
506 unit is correlated down dip to slope turbidite sandstones, interpreted as deposits of flows that  
507 bypassed through the channelised shelf edge rollover. This surface is interpreted as a sequence  
508 boundary without subaerial shelf exposure.

509 In strike section, the older channelised elements are wider, more deeply incised with composite  
510 erosion surfaces filled by amalgamated structureless sandstones, and cut into deeper water facies,  
511 suggesting recurrent erosion and sediment bypass. Younger channel-fills are narrower with cleaner  
512 cuts that incise into shallower water facies, and their fills are better organised with fewer  
513 amalgamation surfaces and basal mudstone clast conglomerates, and more beds with symmetrical  
514 rippled tops. This is consistent with a vertical change to less erosive and shorter lived channels.

515 A gradient increase at the shelf-edge, combined with a high rate of sediment supply associated with  
516 deltaic progradation promoted soft-sediment deformation. Liquefied mixed-influence mouth bars were  
517 susceptible to local remobilisation, and the resulting irregular surfaces likely evolved into subaqueous  
518 sediment conduits. When distributaries reached an unstable and relatively steep region, enhanced  
519 erosion led to larger and deeper incisions across the shelf edge. The interpreted stratigraphic context  
520 and the fact that channels incise into the proximal part of deformed mixed-influence mouth bars  
521 suggest that these subaqueous bodies are the shelf-edge expression of distributary channels,  
522 associated with an abrupt basinward shift of a mixed-influence deltaic system. This study therefore  
523 documents a rare example of the architecture of a progradational mixed-influence paralic succession  
524 superimposed on a shelf edge rollover, in response to a lowering of relative sea level.

525

## 526 **Acknowledgements**

527 The work presented here is part of the SLOPE Project, Phase 4. We thank the consortium of  
528 sponsors (Anadarko, BHPBilliton, BP, CNOOC-Nexen, ConocoPhillips, E.ON, Engie, Maersk,  
529 Murphy, Petrobras, Shell, Statoil, Total, VNG Norge and Woodside) for financial support and strong  
530 scientific engagement. The manuscript benefited from insightful reviews by Gary Hampson, Cornel  
531 Olariu and an anonymous reviewer. Sarah Cobain, Rhodri Jerrett, Eoin Dunlevy and Sascha  
532 Eichenauer are thanked for their collaboration and assistance in the field. Finally, we thank the Karoo  
533 farmers for access to their land.

534

## 535 **References**

536 AINSWORTH, R.B., VAKARELOV, B.K. & NANSON, R.A. 2011. Dynamic spatial and temporal prediction of  
537 changes in depositional processes on clastic shorelines: Toward improved subsurface uncertainty  
538 reduction and management. *AAPG Bulletin*, **95**, 267-297, doi: 10.1306/06301010036.

539 ANDERSSON, P.O.D., WORDEN, R.H., HODGSON, D.M. & FLINT, S. 2004. Provenance evolution and  
540 chemostratigraphy of a Palaeozoic submarine fan-complex: Tanqua Karoo Basin, South Africa.  
541 *Marine and Petroleum Geology*, **21**, 555-577, doi: 10.1016/j.marpetgeo.2004.01.004.

542 BHATTACHARYA, J.P. 2006. Deltas. In: WALKER R.G. & POSAMENTIER H.W. (eds.) *Facies Models*  
543 *revisited*, *SEPM Special Publication*, v. 84, 237-292.

544 BHATTACHARYA, J.P. & GIOSAN, L. 2003. Wave-influenced deltas: geomorphological implications for  
545 facies reconstruction. *Sedimentology*, **50**, 187-210, doi: 10.1046/j.1365-3091.2003.00545.x.

546 BHATTACHARYA, J.P. & MACEACHERN, J.A. 2009. Hyperpycnal rivers and prodeltaic shelves in the  
547 Cretaceous seaway of North America. *Journal of Sedimentary Research*, **79**, 184-209.

548 BOUMA, A.H. & WICKENS, H.D.V. 1991. Permian passive margin submarine fan complex, Karoo Basin.  
549 South Africa: possible model to Gulf of Mexico. *Gulf Coast Association of Geological Societies*  
550 *Transactions*, **41**, 30-42.

551 BOURGET, J., AINSWORTH, R.B. & THOMPSON, S. 2014. Seismic stratigraphy and geomorphology of a  
552 tide or wave dominated shelf-edge delta (NW Australia): Process-based classification from 3D  
553 seismic attributes and implications for the prediction of deep-water sands. *Marine and Petroleum*  
554 *Geology*, **57**, 359-384, doi: <http://dx.doi.org/10.1016/j.marpetgeo.2014.05.021>.

555 BOWMAN, A.P. & JOHNSON, H.D. 2014. Storm-dominated shelf-edge delta successions in a high  
556 accommodation setting: The palaeo-Orinoco Delta (Mayaro Formation), Columbus Basin, South-  
557 East Trinidad. *Sedimentology*, **61**, 792-835, doi: 10.1111/sed.12080.

558 CARVAJAL, C.R. & STEEL, R.J. 2006. Thick turbidite successions from supply-dominated shelves  
559 during sea-level highstand. *Geology*, **34**, 665-668, doi: 10.1130/g22505.1.

560 CARVAJAL, C. & STEEL, R. 2009. Shelf-edge architecture and bypass of sand to deep water: influence  
561 of shelf-edge processes, sea level, and sediment supply. *Journal of Sedimentary Research*, **79**,  
562 652-672, doi: 10.2110/jsr.2009.074.

563 CATTANEO, A., TRINCARDI, F., ASIOLI, A. & CORREGGIARI, A. 2007. The Western Adriatic shelf clinoform:  
564 energy-limited bottomset. *Continental Shelf Research*, **27**, 506-525.

565 CATUNEANU, O., HANCOX, P.J. & RUBIDGE, B.S. 1998. Reciprocal flexural behaviour and contrasting  
566 stratigraphies: a new basin development model for the Karoo retroarc foreland system, South  
567 Africa. *Basin Research*, **10**, 417-439, doi: 10.1046/j.1365-2117.1998.00078.x.

568 CLIFTON, H.E. 2006. A re-examination of facies models for clastic shorelines. *In: POSAMENTIER, H.W. &*  
569 *WALKER, R.G. (eds.) Facies Models Revisited, SEPM Special Publications, vol. 84* 293-337.

570 COLE, D.I. 1992. Evolution and development of the Karoo Basin. *In: DE WIT, M.J. & RANSOME, I.G.D.*  
571 *(eds.) Inversion Tectonics of the Cape Fold Belt, Karoo and Cretaceous Basins of Southern Africa,*  
572 *A.A. Balkema, Rotterdam, 87-99.*

573 COVAULT, J.A., ROMANS, B.W. & GRAHAM, S.A. 2009. Outcrop Expression of a Continental-Margin-  
574 Scale Shelf-Edge Delta from the Cretaceous Magallanes Basin, Chile. *Journal of Sedimentary*  
575 *Research, 79*, 523-539, doi: 10.2110/jsr.2009.053.

576 CRUMEYROLLE, P., RENAUD, I. & SUITER, J. 2007. The use of two- and three-dimensional seismic to  
577 understand sediment transfer from fluvial to deepwater via sinuous channels: example from the  
578 Mahakam shelf and comparison with outcrop data (south central Pyrenees). *Geological Society,*  
579 *London, Special Publications, 277*, 85-103, doi: 10.1144/gsl.sp.2007.277.01.05.

580 DE BEER, C.H. 1992. Structural evolution of the Cape Fold Belt syntaxis and its influence on  
581 syntectonic sedimentation in the SW Karoo Basin. *In: DE WIT, M.J. & RANSOME, I.G.D. (eds.)*  
582 *Inversion Tectonics of the Cape Fold Belt, Karoo and Cretaceous Basins of Southern Africa, A.A.*  
583 *Balkema, Rotterdam, 197-206.*

584 DIXON, J.F., STEEL, R.J. & OLARIU, C. 2012a. River-dominated, shelf-edge deltas: delivery of sand  
585 across the shelf break in the absence of slope incision. *Sedimentology, 59*, 1133-1157, doi:  
586 10.1111/j.1365-3091.2011.01298.x.

587 DIXON, J.F., STEEL, R.J. & OLARIU, C. 2012b. Shelf-edge delta regime as a predictor of deep-water  
588 deposition. *Journal of Sedimentary Research, 82*, 681-687, doi: 10.2110/jsr.2012.59.

589 DONOVAN, A.D. 2003. Depositional topography and sequence development. . *In: ROBERTS, H.H.,*  
590 *ROSEN, N.C., FILLON, R.H. & ANDERSON, J.B. (eds.) Shelf Margin Deltas and linked Down Slope*  
591 *Petroleum Systems: Global Significance and Future Exploration Potential, GCSSEPM Foundation*  
592 *23rd Annual Bob F. Perkins Research Conference, 493-522.*

593 EDWARDS, M.B. 1981. Upper Wilcox Rosita delta system of South Texas; growth-faulted shelf-edge  
594 deltas. *AAPG Bulletin, 65*, 54-73.

595 FAURE, K. & COLE, D. 1999. Geochemical evidence for lacustrine microbial blooms in the vast Permian  
596 Main Karoo, Parana, Falkland Islands and Huab basins of southwestern Gondwana.  
597 *Palaeogeography, Palaeoclimatology, Palaeoecology, 152*, 189-213.

598 FLINT, S. S., HODGSON, D. M., SPRAGUE, A. R., BRUNT, R. L., VAN DER MERWE, W. C., FIGUEIREDO, J.,  
599 PRELAT, A., BOX, D., DI CELMA, C & KAVANAGH, J. P. 2011. Depositional architecture and sequence  
600 stratigraphy of the Karoo basin floor to shelf edge succession, Laingsburg depocentre, South  
601 Africa. *Marine and Petroleum Geology*, **28**(3), 658-674.

602 FULTHORPE, C.S. & AUSTIN, J.A. 1998. Anatomy of rapid margin progradation; three-dimensional  
603 geometries of Miocene clinoforms, New Jersey margin. *AAPG Bulletin*, **82**, 251-273.

604 FULTHORPE, C.S., AUSTIN, J.A. & MOUNTAIN, G.S. 1999. Buried fluvial channels off New Jersey: Did  
605 sea-level lowstands expose the entire shelf during the Miocene? *Geology*, **27**, 203-206, doi:  
606 10.1130/0091-7613(1999)027<0203:bfconj>2.3.co;2.

607 FULTHORPE, C.S., AUSTIN, J.A. & MOUNTAIN, G.S. 2000. Morphology and distribution of Miocene slope  
608 incisions off New Jersey: Are they diagnostic of sequence boundaries? *Geological Society of  
609 America Bulletin*, **112**, 817-828, doi: 10.1130/0016-7606(2000)112<817:madoms>2.0.co;2.

610 GALLOWAY, W.E. 1998. Siliciclastic slope and base-of-slope depositional systems; component facies,  
611 stratigraphic architecture, and classification. *AAPG Bulletin*, **82**, 569-595.

612 HADLER-JACOBSEN, F., JOHANNESSEN, E.P., ASHTON, N., HENRIKSEN, S., JOHNSON, S.D. & KRISTENSEN,  
613 J.B. 2005. Submarine fan morphology and lithology distribution: a predictable function of sediment  
614 delivery, gross shelf-to-basin relief, slope gradient and basin relief/topography. *In: DORÉ, A.G. &  
615 VINING, B.A. (eds.) Petroleum Geology: North West Europe and Global Perspectives, Proceedings  
616 of the 6th Petroleum Geology Conference, London (UK)*, 1121-1145.

617 HAMPSON, G.J. 2000. Discontinuity Surfaces, Clinoforms, and Facies Architecture in a Wave-  
618 Dominated, Shoreface-Shelf Parasequence. *Journal of Sedimentary Research*, **70**, 325-340, doi:  
619 10.1306/2dc40914-0e47-11d7-8643000102c1865d.

620 HAMPSON, G.J. & HOWELL, J.A. 2005. Sedimentologic and geomorphic characterization of ancient  
621 wave-dominated deltaic shorelines; Upper Cretaceous Blackhawk Formation, Book Cliffs, Utah,  
622 U.S.A. *In: GIOSAN, L. & BHATTACHARHYA, J.P. (eds.) River Deltas – Concepts, Models, and  
623 Examples. SEPM Special Publication 83*, 133-154.

624 HELLAND-HANSEN, W. 2010. Facies and stacking patterns of shelf-deltas within the Palaeogene  
625 Battfjellet Formation, Nordenskiöld Land, Svalbard: implications for subsurface reservoir  
626 prediction. *Sedimentology*, **57**, 190-208, doi: 10.1111/j.1365-3091.2009.01102.x.

627 HENRIKSEN, S., HELLAND-HANSEN, W. & BULLIMORE, S. 2011. Relationships between shelf-edge  
628 trajectories and sediment dispersal along depositional dip and strike: a different approach to  
629 sequence stratigraphy. *Basin Research*, **23**, 3-21, doi: 10.1111/j.1365-2117.2010.00463.x.

630 HODGSON, D.M., FLINT, S.S., HODGETTS, D., DRINKWATER, N.J., JOHANNESSEN, E.P. & LUTHI, S.M.  
631 2006. Stratigraphic Evolution of Fine-Grained Submarine Fan Systems, Tanqua Depocenter,  
632 Karoo Basin, South Africa. *Journal of Sedimentary Research*, **76**, 20-40, doi: 10.2110/jsr.2006.03.

633 HUBBARD, S.M., FILDANI, A., ROMANS, B.W., COVAULT, J.A. & MCHARGUE, T.R. 2010. High-relief slope  
634 clinoform development: Insights from outcrop, Magallanes Basin, Chile. *Journal of Sedimentary  
635 Research*, **80**, 357-375, doi: 10.2110/jsr.2010.042.

636 HUTHNANCE, J.M. 1995. Circulation, exchange and water masses at the ocean margin: the role of  
637 physical processes at the shelf edge. *Progress in Oceanography*, **35**, 353-431, doi:  
638 [http://dx.doi.org/10.1016/0079-6611\(95\)80003-C](http://dx.doi.org/10.1016/0079-6611(95)80003-C).

639 IVANOV, V.V., SHAPIRO, G.I., HUTHNANCE, J.M., ALEJNIK, D.L. & GOLOVIN, P.N. 2004. Cascades of  
640 dense water around the world ocean. *Progress in Oceanography*, **60**, 47-98, doi:  
641 <http://dx.doi.org/10.1016/j.pocean.2003.12.002>.

642 JACKSON, C.A.L. & JOHNSON, H.D. 2009. Sustained turbidity currents and their interaction with debrite-  
643 related topography; Labuan Island, offshore NW Borneo, Malaysia. *Sedimentary Geology*, **219**, 77-  
644 96, doi: <http://dx.doi.org/10.1016/j.sedgeo.2009.04.008>.

645 JOHNSON, M.R. 1991. Sandstone petrography, provenance and plate tectonic setting in Gondwana  
646 context of the southeastern Cape-Karoo Basin. *South African Journal of Geology*, **94**, 137-154.

647 JOHNSON, M.R., VAN VUUREN, C.J., VISSER, J.N.J., COLE, D.I., WICKENS, H.D.V., CHRISTIE, A.D.M.,  
648 ROBERTS, D.L. & BRANDL, G. 2006. Sedimentary rocks of the Karoo Supergroup. *In*: JOHNSON,  
649 M.R., ANHAEUSSER, C.R. & THOMAS, R.J. (eds.) *The geology of South Africa*, Geological Society of  
650 South Africa and Council for Geoscience, Pretoria, 461-499.

651 JOHNSON, S.D., FLINT, S., HINDS, D. & DE VILLE WICKENS, H. 2001. Anatomy, geometry and sequence  
652 stratigraphy of basin floor to slope turbidite systems, Tanqua Karoo, South Africa. *Sedimentology*,  
653 **48**, 987-1023.

654 JONES, G.E.D., HODGSON, D.M. & FLINT, S.S. 2013. Contrast in the process response of stacked  
655 clinothems to the shelf-slope rollover. *Geosphere*, **9**, 299-316, doi: 10.1130/ges00796.1.

656 JONES, G.E.D., HODGSON, D.M. & FLINT, S.S. 2015. Lateral variability in clinoform trajectory, process  
657 regime, and sediment dispersal patterns beyond the shelf-edge rollover in exhumed basin margin-  
658 scale clinothems. *Basin Research*, **27**, 657-680.

659 KOLLA, V., BIONDI, P., LONG, B. & FILLON, R. 2000. Sequence stratigraphy and architecture of the Late  
660 Pleistocene Lagniappe delta complex, northeast Gulf of Mexico. *Geological Society, London,*  
661 *Special Publications*, **172**, 291-327, doi: 10.1144/gsl.sp.2000.172.01.14.

662 LEWIS, D.W. 1982. Channels across continental shelves: Corequisites of canyon-fan systems and  
663 potential petroleum conduits. *New Zealand Journal of Geology and Geophysics*, **25**, 209-225, doi:  
664 10.1080/00288306.1982.10421410.

665 LUTHI, S.M., HODGSON, D.M., GEEL, C.R., FLINT, S.S., GOEDBLOED, J.W., DRINKWATER, N.J. &  
666 JOHANESSEN, E.P. 2006. Contribution of research borehole data to modelling fine-grained turbidite  
667 reservoir analogues, Permian Tanqua-Karoo basin floor fans (South Africa). *Petroleum Geology*,  
668 **12**, 175-190.

669 MACQUAKER, J.H.S. & BOHACS, K.M. 2007. On the Accumulation of Mud. *Science*, **318**, 1734-1735,  
670 doi: 10.1126/science.1151980.

671 MATTEUCCI, T.D. & HINE, A.C. 1987. Evolution of the Cape Fear Terrace: A complex interaction  
672 between the Gulf Stream and a paleo-shelf edge delta. *Marine Geology*, **77**, 185-205, doi:  
673 [http://dx.doi.org/10.1016/0025-3227\(87\)90111-3](http://dx.doi.org/10.1016/0025-3227(87)90111-3).

674 MAYALL, M.J., YEILDING, C.A., OLDROYD, J.D., PULHAM, A.J. & SAKURAI, S. 1992. Facies in a shelf-edge  
675 delta; an example from the subsurface of the Gulf of Mexico, middle Pliocene, Mississippi Canyon,  
676 Block 109. *AAPG Bulletin*, **76**, 435-448.

677 MAZIÈRES, A., GILLET, H., CASTELLE, B., GUYOT, C., MULDER, T. & MALLET, C. 2013. Relationship  
678 between longshore drift and the head of the canyon of Capbreton (SW France): descriptive and  
679 numerical approaches. *Proceedings of the 7th International Conference on Coastal Dynamics*, 24-  
680 28 June, Arcachon, France, 1159-1172.

681 MELLERE, D., BREDI, A. & STEEL, R.J. 2003. Fluvial-incised shelf-edge deltas and linkage to upper-  
682 slope channels (Central Tertiary Basin, Spitsbergen). *Shelf-Margin Deltas and Linked Downslope*  
683 *Petroleum Systems: Global Significance and Future Exploration Potential, Gulf Coast Section.*  
684 *23rd Annual Research Conference Houston, Texas*, 231-266.

685 MELLERE, D., PLINK-BJÖRKLUND, P. & STEEL, R.J. 2002. Anatomy of shelf deltas at the edge of a  
686 prograding Eocene shelf margin, Spitsbergen. *Sedimentology*, **49**, 1181-1206.

687 MILTON, N. & DYCE, M. 1995. Systems tract geometries associated with Early Eocene lowstands,  
688 imaged on a 3D seismic dataset from the Bruce area, UK North Sea. in *Steel, R. J.; Felt, V. L.;*  
689 *Johannessen, E. P.; and Mathieu, C., eds. Sequence stratigraphy on the northwest European*  
690 *margin. Norwegian Petroleum Society, Special Publication no. 5*, 429-449.

691 MORTON, R.A. & SUTER, J.R. 1996. Sequence Stratigraphy and Composition of Late Quaternary Shelf-  
692 Margin Deltas, Northern Gulf of Mexico. *AAPG Bulletin*, **80**, 505-530.

693 MOSCARDELLI, L., WOOD, L.J. & DUNLAP, D.B. 2012. Shelf-edge deltas along structurally complex  
694 margins: A case study from eastern offshore Trinidad. *AAPG Bulletin*, **96**, 1483-1522, doi:  
695 10.1306/01241211046.

696 MULDER, T., SYVITSKI, J.P.M., MIGEON, S., FAUGÈRES, J.C. & SAVOYE B. 2003. Hyperpycnal turbidity  
697 currents: initiation, behavior and related deposits: a review. *Marine and Petroleum Geology* **20**,  
698 861-882.

699 MUTO, T. & STEEL, R.J. 2002. In Defense of Shelf Edge Delta Development during Falling and  
700 Lowstand of Relative Sea Level. *The Journal of Geology*, **110**, 421-436, doi: 10.1086/340631.

701 MUTTI, E., TINTERRI, R., BENEVELLI, G., DIBIASE, D. & CAVANNA, G. 2003. Deltaic, mixed and turbidite  
702 sedimentation of ancient foreland basins. *Turbidites: Models and Problems (Eds E. Mutti, G.S.*  
703 *Steffens, C. Pirmez, M. Orlando and D. Roberts)*, *Marine and Petroleum Geology*, **20**, 733-755.

704 NORMANDEAU, A., LAJEUNESSE, P., ST-ONGE, G., BOURGAULT, D., DROUIN, S.S.-O., SENNEVILLE, S. &  
705 BELANGER, S. 2014. Morphodynamics in sediment-starved inner-shelf submarine canyons (Lower  
706 St. Lawrence Estuary, Eastern Canada). *Marine Geology*, **357**, 243-255, doi:  
707 <http://dx.doi.org/10.1016/j.margeo.2014.08.012>.

708 NØTTVEDT, A. & KREISA, R.D. 1987. Model for the combined-flow origin of hummocky cross-  
709 stratification. 357-361.

710 OLARIU, C. 2014. Autogenic process change in modern deltas. *From Depositional Systems to*  
711 *Sedimentary Successions on the Norwegian Continental Margin*. John Wiley & Sons, Ltd, 149-166.

712 OLARIU, C. & BHATTACHARYA, J.P. 2006. Terminal distributary channels and delta front architecture of  
713 river-dominated delta systems. *Journal of Sedimentary Research*, **76**, 212-233, doi:  
714 10.2110/jsr.2006.026.

715 OLARIU, C. & STEEL, R.J. 2009. Influence of point-source sediment-supply on modern shelf-slope  
716 morphology: implications for interpretation of ancient shelf margins. *Basin Research*, **21**, 484-501,  
717 doi: 10.1111/j.1365-2117.2009.00420.x.

718 OLARIU, C., STEEL, R.J. & PETTER, A.L. 2010. Delta-front hyperpycnal bed geometry and implications  
719 for reservoir modeling: Cretaceous Panther Tongue delta, Book Cliffs, Utah. *AAPG Bulletin*, **94**,  
720 819-845.

721 OLARIU, M.I., CARVAJAL, C.R., OLARIU, C. & STEEL, R.J. 2012. Deltaic process and architectural  
722 evolution during cross-shelf transits, Maastrichtian Fox Hills Formation, Washakie Basin,  
723 Wyoming. *AAPG Bulletin*, **96**, 1931-1956.

724 OLIVEIRA, C.M.M., HODGSON, D.M. & FLINT, S.S. 2011. Distribution of soft-sediment deformation  
725 structures in clinoform successions of the Permian Ecca Group, Karoo Basin, South Africa.  
726 *Sedimentary Geology*, **235**, 314-330.

727 OWEN, G. 2003. Load structures: gravity-driven sediment mobilization in the shallow subsurface.  
728 *Geological Society, London, Special Publications*, **216**, 21-34, doi: 10.1144/gsl.sp.2003.216.01.03.

729 PATRUNO, S., HAMPSON, G.J. & JACKSON, C.A.L. 2015. Quantitative characterisation of deltaic and  
730 subaqueous clinoforms. *Earth-Science Reviews*, **142**, 79-119, doi:  
731 <http://dx.doi.org/10.1016/j.earscirev.2015.01.004>.

732 PATTISON, S.A. 2005. Storm-influenced prodelta turbidite complex in the Lower Kenilworth Member at  
733 Hatch Mesa, Book Cliffs, Utah, USA: implications for shallow marine facies models. *Journal of*  
734 *Sedimentary Research*, **75**, 420-439.

735 PATTISON, S.A., BRUCE AINSWORTH, R. & HOFFMAN, T.A. 2007. Evidence of across-shelf transport of  
736 fine-grained sediments: turbidite-filled shelf channels in the Campanian Aberdeen Member, Book  
737 Cliffs, Utah, USA. *Sedimentology*, **54**, 1033-1064.

738 PETTER, A.L. & STEEL, R.J. 2005. Deepwater-slope channels and hyperpycnal flows from the Eocene  
739 of the central Spitsbergen Basin: Predicting basin-floor sands from a shelf edge/upper slope  
740 perspective. *AAPG Annual Meeting, June 19–22, 2005, Calgary, Alberta*.

741 PETTER, A.L. & STEEL, R.J. 2006. Hyperpycnal flow variability and slope organization on an Eocene  
742 shelf margin, Central Basin, Spitsbergen. *AAPG Bulletin*, **90**, 1451-1472.

743 PIRMEZ, C., PRATSON, L.F. & STECKLER, M.S. 1998. Clinof orm development by advection-diffusion of  
744 suspended sediment: Modeling and comparison to natural systems. *Journal of Geophysical*  
745 *Research*, **103**, 24141-24157, doi: 10.1029/98jb01516.

746 PLINK-BJÖRKLUND, P. & STEEL, R. 2002. Sea-level fall below the shelf edge, without basin-floor fans.  
747 *Geology*, **30**, 115-118.

748 PLINK-BJÖRKLUND, P. & STEEL, R.J. 2004. Initiation of turbidity currents: Outcrop evidence for Eocene  
749 hyperpycnal flow turbidites. *Sedimentary Geology*, **165**, 29-52.

750 PLINK-BJÖRKLUND, P. & STEEL, R. 2005. Deltas on falling-stage and lowstand shelf margins, the  
751 Eocene Central Basin of Spitsbergen: importance of sediment supply. In: GIOSAN, L. &  
752 BHATTACHARYA, J.P. (eds.) *River Deltas - Concepts, Models, and Examples*, SEPM, *Special*  
753 *Publication 83*, 179-206.

754 POAG, C.W., SWIFT, B.A., SCHLEE, J.S., BALL, M.M. & SHEETZ, L.L. 1990. Early Cretaceous shelf-edge  
755 deltas of the Baltimore Canyon Trough: Principal sources for sediment gravity deposits of the  
756 northern Hatteras Basin. *Geology*, **18**, 149-152, doi: 10.1130/0091-  
757 7613(1990)018<0149:ecsedo>2.3.co;2.

758 PONTÉN, A. & PLINK-BJÖRKLUND, P. 2009. Process Regime Changes Across a Regressive to  
759 Transgressive Turnaround in a Shelf–Slope Basin, Eocene Central Basin of Spitsbergen. *Journal*  
760 *of Sedimentary Research*, **79**, 2-23, doi: 10.2110/jsr.2009.005.

761 PORĘBSKI, S.J. & STEEL, R.J. 2003. Shelf-margin deltas: their stratigraphic significance and relation to  
762 deepwater sands. *Earth-Science Reviews*, **62**, 283-326.

763 PORĘBSKI, S.J. & STEEL, R.J. 2006. Deltas and sea-level change. *Journal of Sedimentary Research*,  
764 **76**, 390-403.

765 POSAMENTIER, H.W., JERVEY, M.T. & VAIL, P.R. 1988. Eustatic controls on clastic deposition I -  
766 conceptual framework. in C.K. Wilgus, B.S. Hastings, C.G.S.C. Kendall, H.W. Posamentier, C.A.  
767 Ross and J.C. Van Wagoner eds., *Sea Level Changes - An Integrated Approach*, SEPM *Special*  
768 *Publication*, **42**.

769 POSAMENTIER, H.W. & KOLLA, V. 2003. Seismic Geomorphology and Stratigraphy of Depositional  
770 Elements in Deep-Water Settings. *Journal of Sedimentary Research*, **73**, 367-388, doi:  
771 10.1306/111302730367.

772 PRATSON, L.F., RYAN, W.B.F., MOUNTAIN, G.S. & TWICHELL, D.C. 1994. Submarine canyon initiation by  
773 downslope-eroding sediment flows: Evidence in late Cenozoic strata on the New Jersey  
774 continental slope. *Geological Society of America Bulletin*, **106**, 395-412, doi: 10.1130/0016-  
775 7606(1994)106<0395:scibde>2.3.co;2.

776 PRÉLAT, A., PANKHANIA SHYAM, S., JACKSON, C., A-L. & HODGSON, D.M. 2015. Slope gradient and  
777 lithology as controls on the initiation of submarine slope gullies; insights from the North Carnarvon  
778 Basin, Offshore NW Australia. *Sedimentary Geology*, doi:  
779 <http://dx.doi.org/10.1016/j.sedgeo.2015.08.009>.

780 PYLES, D.R. & SLATT, R.M. 2000. A high-frequency sequence stratigraphic framework for the shallow  
781 through deep-water deposits of the Lewis Shale and Fox Hills Sandstone, Great Divide and  
782 Washakie basins, Wyoming. In: WEIMER, P., SLATT, R.M., COLEMAN, J., ROSEN, N.C., NELSON, C.H.,  
783 BOUMA, A.H., STYZEN, M.J. & LAWRENCE, D.T. (eds.) *Deep-Water Reservoirs of the World, SEPM,*  
784 *Gulf Coast Section, 20th Annual Research Conference, Houston, Texas*, 836-861.

785 PYLES, D.R. & SLATT, R.M. 2007. Applications to understanding shelf edge to base-of-slope changes  
786 in stratigraphic architecture of prograding basin margins: Stratigraphy of the Lewis Shale,  
787 Wyoming, USA. In: NILSEN, T.H., SHEW, R.D., STEFFENS, G.S. & STUDLICK, J.R.J. (eds.) *Atlas of*  
788 *Deepwater Outcrops: AAPG Studies in Geology* 56, 485-489.

789 RIDENTE, D., FOGLINI, F., MINISINI, D., TRINCARDI, F. & VERDICCHIO, G. 2007. Shelf-edge erosion,  
790 sediment failure and inception of Bari Canyon on the Southwestern Adriatic Margin (Central  
791 Mediterranean). *Marine Geology*, **246**, 193-207, doi:  
792 <http://dx.doi.org/10.1016/j.margeo.2007.01.014>.

793 ROSS, W.C., HALLIWELL, B.A., MAY, J.A., WATTS, D.E. & SYVITSKI, J.P.M. 1994. Slope readjustment: a  
794 new model for the development of submarine fans and aprons. *Geology*, **22**, 511-514.

795 RUBIN, D.M. & MCCULLOCH, D.S. 1980. Single and superimposed bedforms: a synthesis of San  
796 Francisco Bay and flume observations. *Sedimentary Geology*, **26**, 207-231.

797 RYAN, M.C., HELLAND-HANSEN, W., JOHANNESSEN, E.P. & STEEL, R.J. 2009. Erosional vs. accretionary  
798 shelf margins: the influence of margin type on deepwater sedimentation: an example from the  
799 Porcupine Basin, offshore western Ireland. *Basin Research*, **21**, 676-703, doi: 10.1111/j.1365-  
800 2117.2009.00424.x.

801 SALLER, A.H., NOAH, J.T., RUZUAR, A.P. & SCHNEIDER, R. 2004. Linked lowstand delta to basin-floor  
802 fan deposition, offshore Indonesia: An analog for deep-water reservoir systems. *AAPG Bulletin*,  
803 **88**, 21-46, doi: 10.1306/09030303003.

804 SANCHEZ, C.M., FULTHORPE, C.S. & STEEL, R.J. 2012a. Middle Miocene–Pliocene siliciclastic influx  
805 across a carbonate shelf and influence of deltaic sedimentation on shelf construction, Northern  
806 Carnarvon Basin, Northwest Shelf of Australia. *Basin Research*, **24**, 664-682, doi: 10.1111/j.1365-  
807 2117.2012.00546.x.

808 SANCHEZ, C.M., FULTHORPE, C.S. & STEEL, R.J. 2012b. Miocene shelf-edge deltas and their impact on  
809 deepwater slope progradation and morphology, Northwest Shelf of Australia. *Basin Research*, **24**,  
810 683-698, doi: 10.1111/j.1365-2117.2012.00545.x.

811 SCHIEBER, J., SOUTHARD, J. & THAISEN, K. 2007. Accretion of Mudstone Beds from Migrating Floccule  
812 Ripples. *Science*, **318**, 1760-1763, doi: 10.1126/science.1147001.

813 SCOTT, E.D., BOUMA, A.H. & WICKENS, H.D.V. 2000. Influence of tectonics on submarine fan  
814 deposition, Tanqua and Laingsburg subbasins, South Africa. *In*: A.H., B. & STONE, C.G. (eds.)  
815 *Fine-grained turbidite systems, American Association of Petroleum Geologists Memoir 72*, 47-56.

816 SHAPIRO, G.I. & HILL, A.E. 1997. Dynamics of Dense Water Cascades at the Shelf Edge. *Journal of*  
817 *Physical Oceanography*, **27**, 2381-2394, doi: 10.1175/1520-  
818 0485(1997)027<2381:dodwca>2.0.co;2.

819 SMITH, R.M.H. 1990. A review of stratigraphy and sedimentary environments of the Karoo Basin of  
820 South Africa. *Journal of African Earth Sciences (and the Middle East)*, **10**, 117-137, doi:  
821 [http://dx.doi.org/10.1016/0899-5362\(90\)90050-O](http://dx.doi.org/10.1016/0899-5362(90)90050-O).

822 SOUTHARD, J.B. 1971. Representation of bed configurations in depth-velocity-size diagrams. *Journal*  
823 *of Sedimentary Petrology*, **41**, 903-915.

824 SOUTHARD, J.B. & BOGUCHWAL, L.A. 1990. Bed configurations in steady unidirectional water flows.  
825 Part 2. Synthesis of flume data. *Journal of Sedimentary Research*, **60**, 658-679.

826 SOUTHARD, J.B., LAMBIE, J.M., FEDERICO, D.C., PILE, H.T. & WEIDMAN, C.R. 1990. Experiments on bed  
827 configurations in fine sands under bidirectional purely oscillatory flow, and the origin of hummocky  
828 cross-stratification. *Journal of Sedimentary Research*, **60**, 1-17, doi: 10.1306/212f90f7-2b24-11d7-  
829 8648000102c1865d.

830 STEAR, W.M. 1983. Morphological characteristics of ephemeral stream channel and overbanks splay  
831 sandstone bodies in the Permian Lower Beaufort Group, Karoo Basin, South Africa. *In: COLLINSON,*  
832 *J.D. & LEWIN, J. (eds.) Modern and Ancient Fluvial Systems: International Association of*  
833 *Sedimentologists, Special Publication 6, 405-420.*

834 STEAR, W.M. 1985. Comparison of the bedform distribution and dynamics of modern and ancient  
835 sandy ephemeral flood deposits in the southwestern Karoo region, South Africa. *Sedimentary*  
836 *Geology, 45, 209-230.*

837 STEEL, R.J., CRABAUGH, J., SCHELPEPPER, M., MELLERE, D., PLINK-BJÖRKLUND, P., DEIBERT, J. &  
838 LØSETH, T. 2000. Deltas vs. rivers on the shelf edge: their relative contributions to the growth of  
839 shelf-margins and basin-floor fans (Barremian and Eocene, Spitsbergen). *GCSSEPM Foundation*  
840 *20th Annual Bob F. Perkins Research Conference, 981–1009.*

841 STEEL, R.J., POREBSKI, S.J., PLINK-BJORKLUND, P., MELLERE, D. & SCHELLPEPER, M. 2003. Shelf-edge  
842 delta types and their sequence-stratigraphic relationships. *Shelf Margin Deltas and Linked Down*  
843 *Slope Petroleum Systems: Global Significance and Future Exploration Potential, Houston, Texas.*  
844 *December 7-10., 205-230.*

845 STEVENSON, C.J., JACKSON, C.A.-L., HODGSON, D.M., HUBBARD, S.M. & EGGENHUISEN, J.T. 2015.  
846 Deep-water sediment bypass. *Journal of Sedimentary Research, 85, 1058-1081.*

847 SUTER, J.R. & BERRYHILL, H.L. 1985. Late Quaternary shelf-margin deltas, Northwest Gulf of Mexico.  
848 *AAPG Bulletin, 69, 77-91.*

849 SYDOW, J. & ROBERTS, H.H. 1994. Stratigraphic framework of a late Pleistocene shelf-edge delta,  
850 Northeast Gulf of Mexico. *AAPG Bulletin, 78, 1276-1312.*

851 SYLVESTER, Z., DEPTUCK, M.E., PRATHER, B.E., PIRMEZ, C. & O'BYRNE, C. 2012. Seismic Stratigraphy  
852 of a Shelf-Edge Delta and Linked Submarine Channels in the Northeastern Gulf of Mexico. *In:*  
853 *PRATHER, B., DEPTUCK, M.E., MOHRIG, D., VAN HOOR, B. & WYNN, R.B. (eds.) Application of the*  
854 *Principles of Seismic Geomorphology to Continental-Slope and Base-of-Slope Systems: Case*  
855 *Studies from Seafloor and Near-Seafloor Analogues, SEPM Society for Sedimentary Geology*  
856 *Special Publication, 99, 31-59.*

857 TALLING, P.J. 1998. How and where do incised valleys form if sea level remains above the shelf edge?  
858 *Geology, 26, 87-90, doi: 10.1130/0091-7613(1998)026<0087:hawdiv>2.3.co;2.*

859 TANKARD, A., WELSINK, H., AUKE, P., NEWTON, R. & STETTLER, E. 2009. Tectonic evolution of the  
860 Cape and Karoo basins of South Africa. *Marine and Petroleum Geology*, **26**, 1379-1412, doi:  
861 10.1016/j.marpetgeo.2009.01.022.

862 TESSON, M., GENSOUS, B., ALLEN, G.P. & RAVENNE, C. 1990. Late Quaternary deltaic lowstand wedges  
863 on the Rhône continental shelf, France. *Marine Geology*, **91**, 325-332, doi:  
864 [http://dx.doi.org/10.1016/0025-3227\(90\)90053-M](http://dx.doi.org/10.1016/0025-3227(90)90053-M).

865 TINTERI, R. 2007. The lower Eocene Roda Sandstone (South-Central Pyrenees): an example of a  
866 flood-dominated river-delta system in a tectonically controlled basin. *Rivista Italiana di*  
867 *Paleontologia e Stratigrafia*, **113**, 223-255.

868 TURNER, B.R. 1981. Possible origin of low angle cross-strata and horizontal lamination in Beaufort  
869 Group sandstones of the southern Karoo Basin. *Geological Society of South Africa, Transactions*,  
870 **84**, 193-197.

871 TURNER, B.R. 1999. Tectonostratigraphical development of the Upper Karoo foreland basin: Orogenic  
872 unloading versus thermally-induced Gondwana rifting. *Journal of African Earth Sciences*, **28**, 215-  
873 238.

874 UROZA, C.A. & STEEL, R.J. 2008. A highstand shelf-margin delta system from the Eocene of West  
875 Spitsbergen, Norway. *Sedimentary Geology*, **203**, 229-245.

876 VAN DEN BERG, J.H. & VAN GELDER, A. 1993. A new bedform stability diagram, with emphasis on the  
877 transition of ripples to plane bed in flows over fine sand and silt. In: MARZO, M. & PUIGDEFABREGAS,  
878 C. (eds.) *Alluvial Sedimentation, International Association of Sedimentologists, Special Publication*  
879 *17*, 11-21.

880 VAN DER WERFF, W. & JOHNSON, S. 2003. High resolution stratigraphic analysis of a turbidite system,  
881 Tanqua Karoo Basin, South Africa. *Marine and Petroleum Geology*, **20**, 45-69, doi:  
882 [http://dx.doi.org/10.1016/S0264-8172\(03\)00025-4](http://dx.doi.org/10.1016/S0264-8172(03)00025-4).

883 VAN WAGONER, J.C., MITCHUM, R.M., CAMPION, K.M. & RAHMANIAN, V.D. 1990. Siliciclastic sequence  
884 stratigraphy in well logs, cores, and outcrops. American Association of Petroleum Geologists  
885 Methods in Exploration Series, No. 7, Tulsa, Oklahoma.

886 VEEVERS, J.J., COLE, D.I. & COWAN, E.J. 1994. Southern Africa: Karoo Basin and Cape Fold Belt. In:  
887 VEEVERS, J.J. & POWELL, C.M. (eds.) *Permian-Triassic Pangean basins and foldbelts along the*  
888 *Panthalassan Margin of Gondwanaland. Geological Society America Memoir 184*, 223-279.

889 VIANA, A.R., HERCOS, C.M., DE ALMEIDA, W., MAGALHÃES, J.L. & DE ANDRADE, S.B. 2002. Evidence of  
890 bottom current influence on the Neogene to Quaternary sedimentation along the northern Campos  
891 Slope, SW Atlantic Margin. *In: STOW, D.A.V., FAUGÈRES, J.-C., PUDSEY, C.J., HOWE, J.A. & VIANA,*  
892 *A.R. (eds.) Deep-Water Contourite Systems: Modern Drifts and Ancient Series, Seismic and*  
893 *Sedimentary Characteristics. Geological Society, London, Memoir 22, 249-259.*

894 VISSER, J.N.J. 1993. Sea-level changes in a back-arc-foreland transition: the late Carboniferous-  
895 Permian Karoo Basin of South Africa. *Sedimentary Geology*, **83**, 115-131, doi:  
896 [http://dx.doi.org/10.1016/0037-0738\(93\)90185-8](http://dx.doi.org/10.1016/0037-0738(93)90185-8).

897 WICKENS, H.D.V. 1994. Basin Floor Fan Building Turbidites of the Southwestern Karoo Basin, Permian  
898 Ecca Group, South Africa. [unpublished Ph.D. Thesis]. *University of Port Elizabeth, Port Elizabeth*  
899 *(South Africa)*, 233.

900 WILD, R. 2005. *Sedimentological and sequence stratigraphic evolution of a Permian lower slope to*  
901 *shelf succession, Tanqua depocentre, SW Karoo Basin, South Africa. PhD Thesis, University of*  
902 *Liverpool.*

903 WILD, R., FLINT, S.S. & HODGSON, D.M. 2009. Stratigraphic evolution of the upper slope and shelf  
904 edge in the Karoo Basin, South Africa. *Basin Research*, **21**, 502-527.

905 WILD, R., HODGSON, D.M. & FLINT, S.S. 2005. Architecture and stratigraphic evolution of multiple,  
906 vertically-stacked slope channel complexes, Tanqua depocentre, Karoo Basin, South Africa. *In:*  
907 *HODGSON, D.M. & FLINT, S.S. (eds.) Submarine Slope Systems: Processes and Products.*  
908 *Geological Society of London Special Publication 244*, 89-111.

909 WILSON, A., FLINT, S., PAYENBERG, T., TOHVER, E. & LANCI, L. 2014. Architectural Styles and  
910 Sedimentology of the Fluvial Lower Beaufort Group, Karoo Basin, South Africa. *Journal of*  
911 *Sedimentary Research*, **84**, 326-348, doi: 10.2110/jsr.2014.28.

912 WILSON, P.A. & ROBERTS, H.H. 1995. Density cascading: off-shelf sediment transport, evidence and  
913 implications, Bahama Banks. *Journal of Sedimentary Research*, **65**, 45-56, doi:  
914 10.1306/d426801d-2b26-11d7-8648000102c1865d.

915 ZAVALA, C., ARCURI, M., DI MEGLIO, M., GAMERO, H. & CONTRERAS, C. 2011. A genetic facies tract for  
916 the analysis of sustained hyperpycnal flow deposits. *In: SLATT, R.M. & ZAVALA, C. (eds.) Sediment*  
917 *transfer from shelf to deep water - Revisiting the delivery system. AAPG Studies in Geology 61*, 1-  
918 21.

919

920

921

922 **Figure captions**

923

924 Fig. 1: (a) The southwestern Karoo Basin with Tanqua and Laingsburg depocentres outlined. (b) The  
925 Tanqua depocentre study area. (c) Detailed map of the Paardeberg Ridge locality. Log positions are  
926 shown in white, and black lines indicate mapped erosion surfaces. Images from Google Earth.

927

928 Fig. 2: (a) Summary stratigraphy of the Tanqua Depocentre adapted from Wickens (1994), Wild *et al.*  
929 (2009) and Flint *et al.* (2011). The Waterford Formation here includes the Kookfontein Formation. (b)  
930 Summary log (DRs in Fig.1c) of the Paardeberg Ridge succession. The middle unit is the focus of this  
931 work

932

933 Fig. 3: (a) Vertically exaggerated photo-panorama of the SW face of the Paardeberg Ridge. Log  
934 positions are shown in white. (b) Architectural detail of the middle unit. Black lines mark the contacts  
935 between different elements and red dotted lines show the positions of mudstone clast lags. All  
936 depositional elements have been coded, for example t1C or t4L, where “t1” or “t4” is related to the  
937 relative time of deposition, inferred from the lateral and vertical relationships between the elements.  
938 “C” or “L” refers to channelised or lobate body. The oldest erosion surface (t1<sub>C</sub>) that truncates distal  
939 prodelta facies of the uppermost slope parasequences is interpreted as the basal sequence boundary  
940 of the middle unit.

941

942 Fig. 4: Rose diagrams showing palaeocurrent distribution for the (a) lower, middle and upper units;  
943 and comparing (b) channelised vs. (c) lobate bodies, showing measurements within the different parts  
944 of the elements; (d) types of measurements. Dark colour represents bidirectional measurements while  
945 light colour represents unidirectional measurements. Def = deformation.

946

947 Fig. 5: Representative photographs of lithofacies from the middle unit. Table 1 outlines the lithofacies  
948 codes and interpretation of depositional processes (Ci: Matrix- to clast-supported intraformational

949 conglomerate; Cm: Mudstone clast horizon; Ss: Structureless sandstone; Sr: Ripple or climbing  
950 ripple-lamination; Sg: Inverse to normal graded sandstone; Sp: Parallel bedded sandstone; Sx: High  
951 angle planar or trough-cross bedded sandstone Sw: wavy lamination and symmetrical ripple-  
952 lamination).

953

954 Fig. 6: Dimensions, geometries and facies associations observed by depositional element, for  
955 channelised bodies (symmetric, asymmetric or amalgamated fills) and lobate bodies. Sd: Sandstone;  
956 St: Siltstone. Below: Summary table of width, thickness and length (“>” maximum measured due to  
957 outcrop constrains) values for the channelised and lobate elements measured in the Paardeberg  
958 ridge.

959

960 Fig. 7: Map of the channelised elements from SW to NE of the Paardeberg Ridge. Black lines  
961 represent mapped erosion surfaces. Dotted lines represent correlative surfaces between the two  
962 sides of the Paardeberg Ridge. Arrows represent main palaeocurrents. Right hand side table  
963 summarise the differences observed comparing the elements in up dip and down dip positions.

964

965 Fig. 8: Idealised geometrical relationships observed between channelised and lobate elements in  
966 strike section. Colour code is the same as in Figures 3 and 6. Left log shows a lobe element cut by a  
967 channelised element and overlain by the off-axis part of another lobate element (triangles in the  
968 middle of the figure represent the position of the log). Right log shows two lobe elements (triangles on  
969 the right show position of the log).

970

971 Fig. 9: (a) Photograph and correlation between DR6, 7 & 8 between the SW and NE faces of the  
972 ridge, showing down dip deepening and thickening of the channel. Palaeocurrents are parallel with  
973 the exposure. \*1,2,3,4 mark key surfaces. (b) Geometrical relationships between channelised and  
974 lobate bodies from up-dip (SW) to down-dip (NE). Colour code as for Figure 3 and 6. Blue colour  
975 represents bidirectional measurements while green colour represents unidirectional measurements

976

977 Fig. 10: Walked out correlation between DR1, DR6 and the OUS section, 2 km down dip. The top of  
978 the OUS section is interpreted as turbidites deposited from flows that bypassed the channelised shelf-

979 edge rollover. Outcrop photographs (a) and (b) show details of the erosion down dip. Blue lines  
980 represent regional flooding surfaces and the red line is the correlation of the basal sequence  
981 boundary of the middle unit.

982

983 Fig. 11: a) Synthesis of observations and interpretations, showing generalised vertical and lateral  
984 stacking of depositional elements for a prograding mixed-influence shelf edge rollover. Note the  
985 stratigraphic decrease in channel size. b) Detail of a channel morphology in this setting.

986

987 Table 1: Facies classification, description and process interpretations of the middle unit.

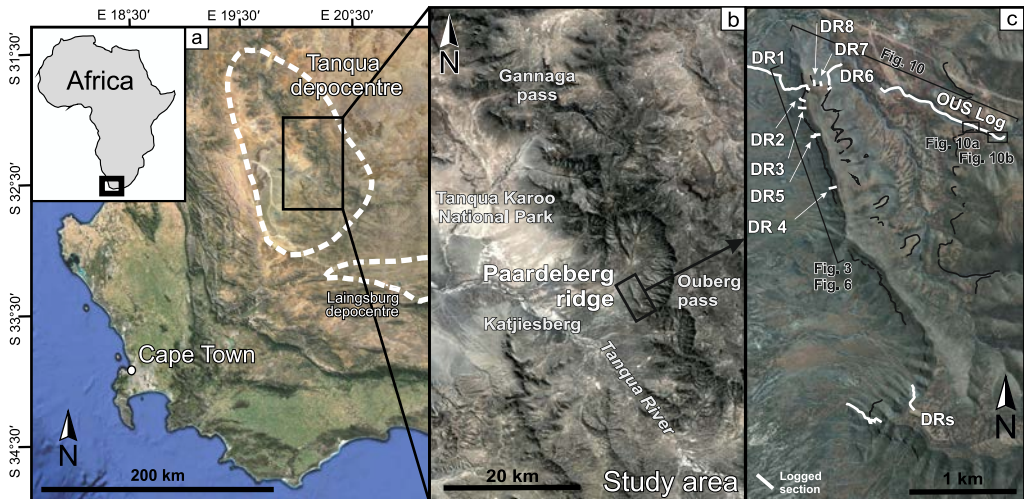


Fig.1

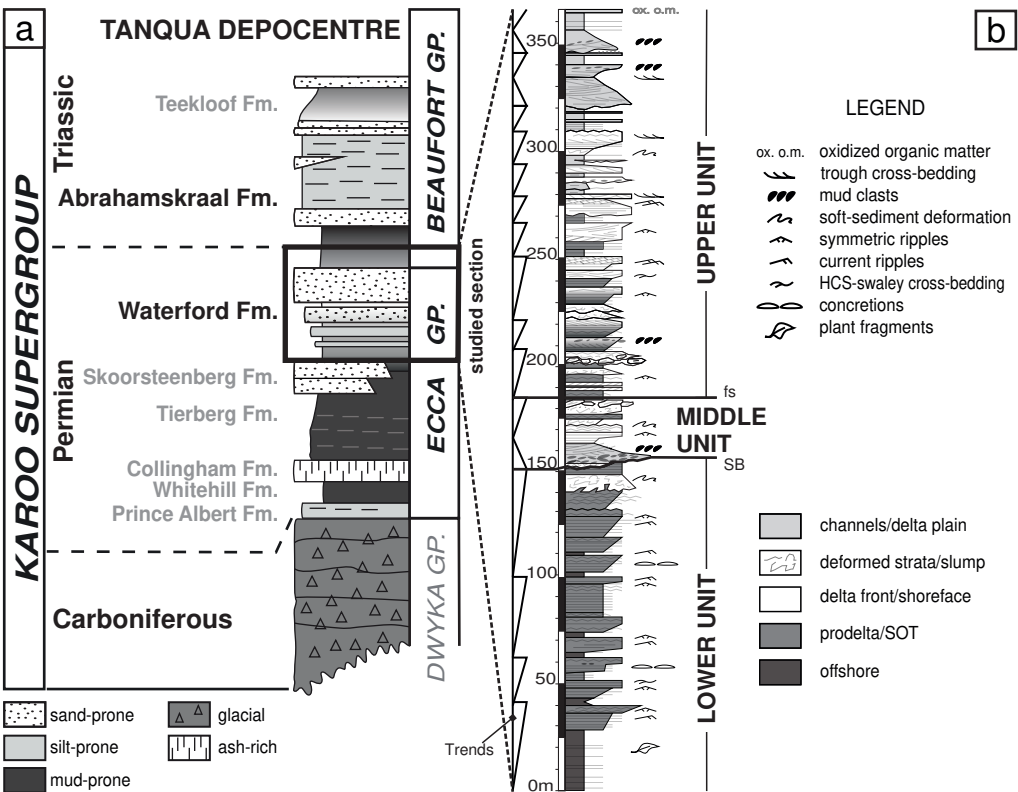


Fig.2

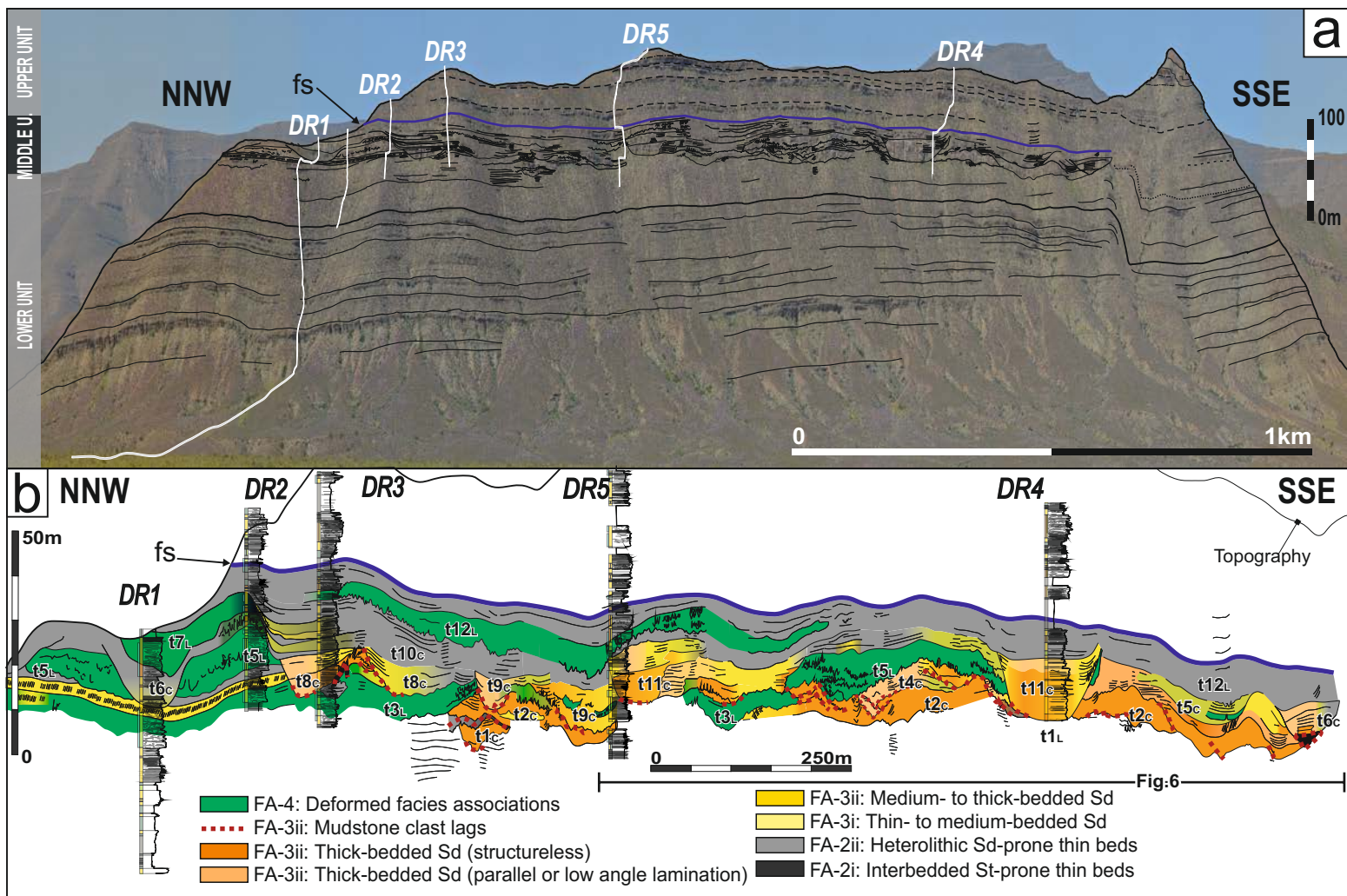


Fig.3

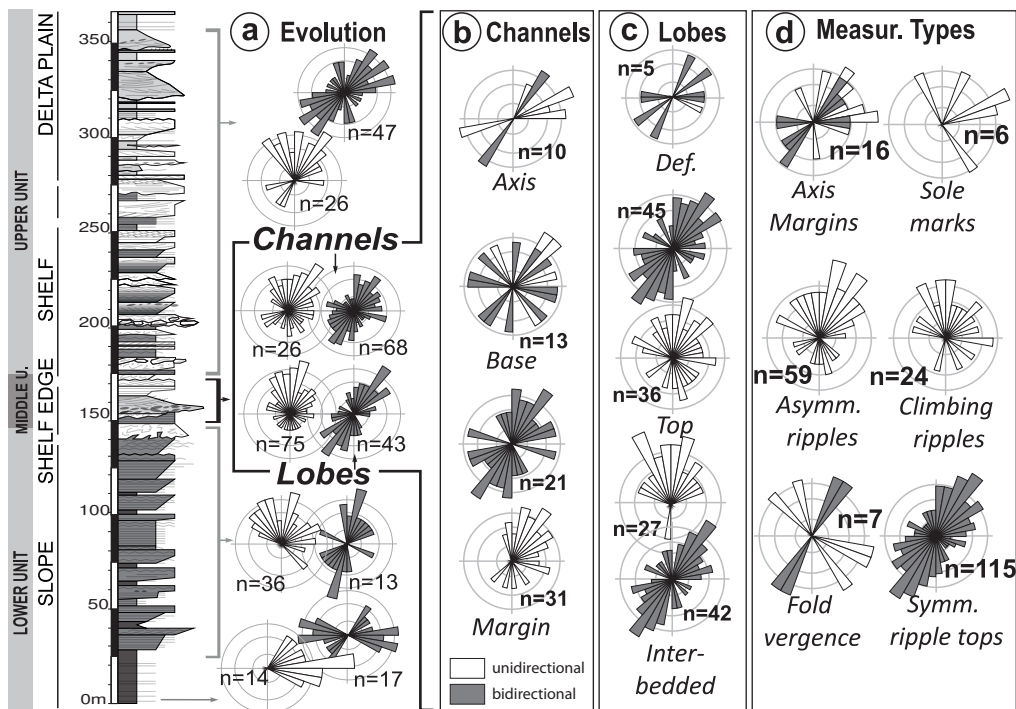


Fig.4

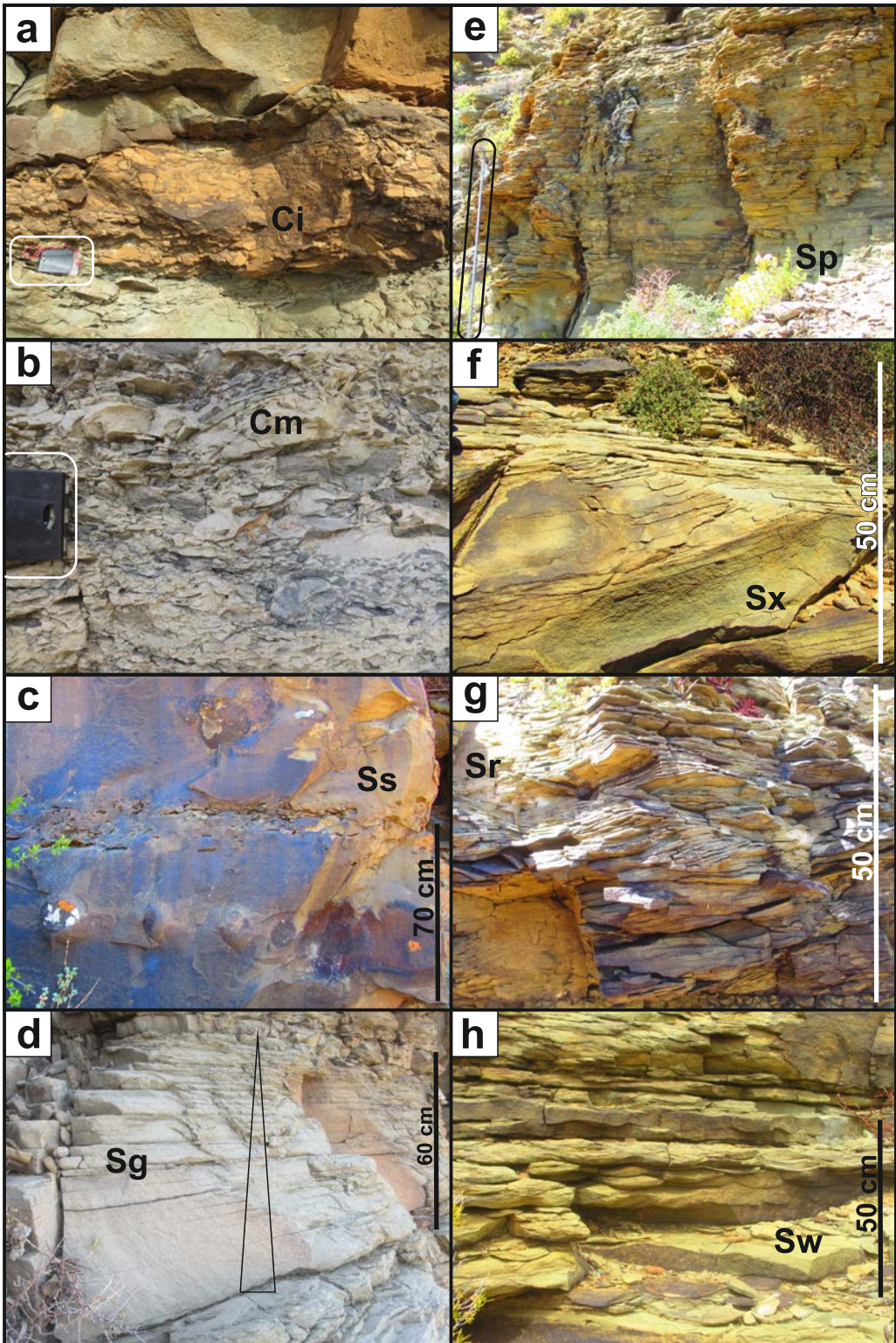


Fig5.

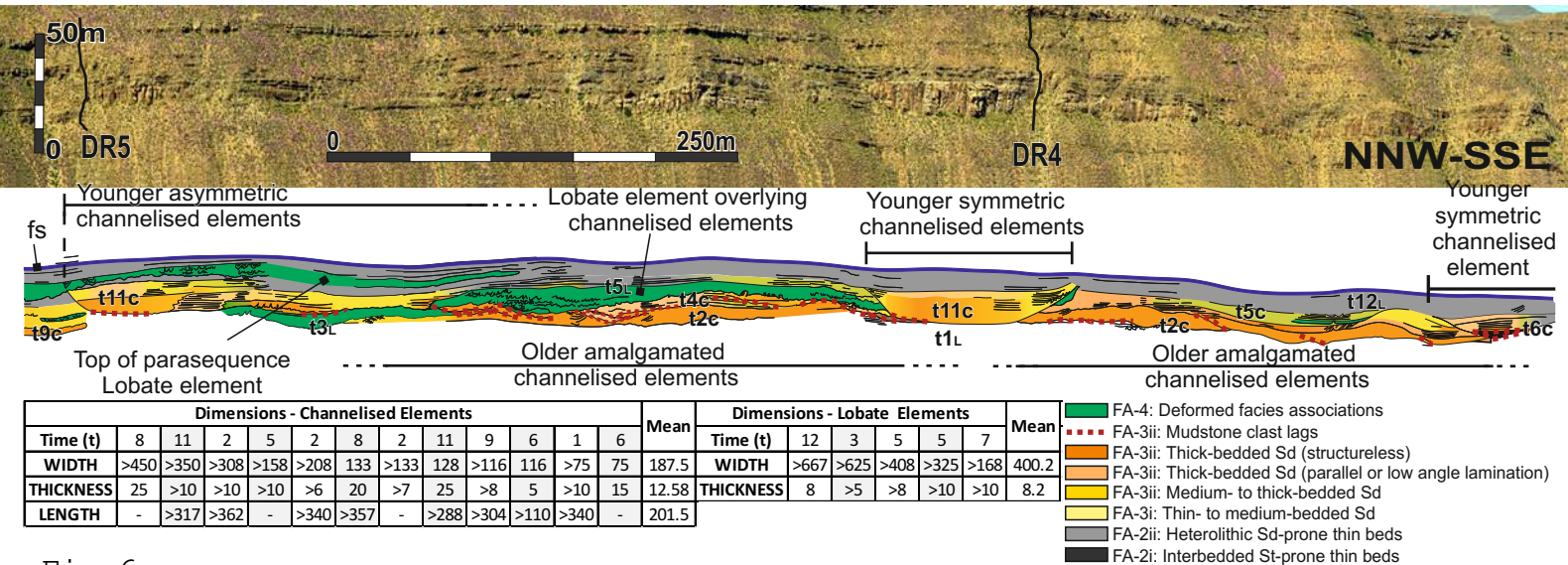
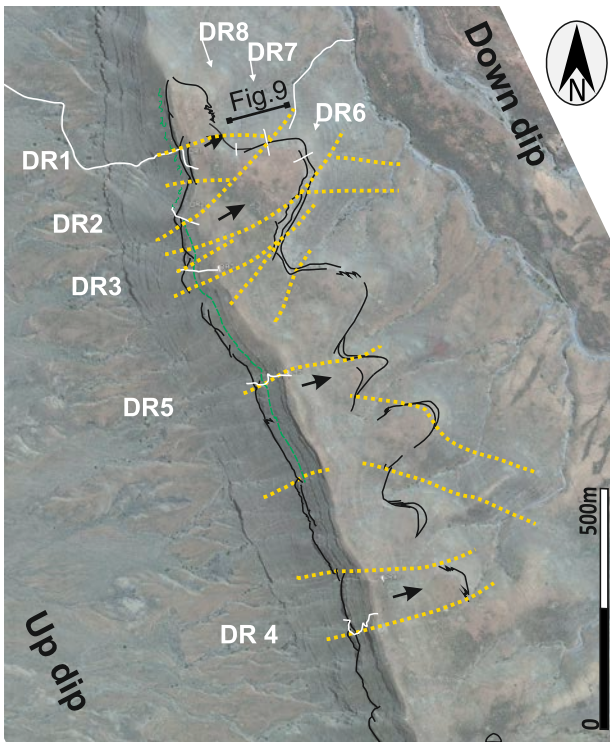


Fig.6



	Channels	
	SW	NE
	up dip	down dip
Thickness	thinner	thicker
Incision/ erosion	less deep	more deeply incised
Mud dast lags	less	more
Soft sediment deformation	less	more
Cutting/ Facies eroded	shallower facies: delta front or other channels	deeper facies: prodelta

Fig.7



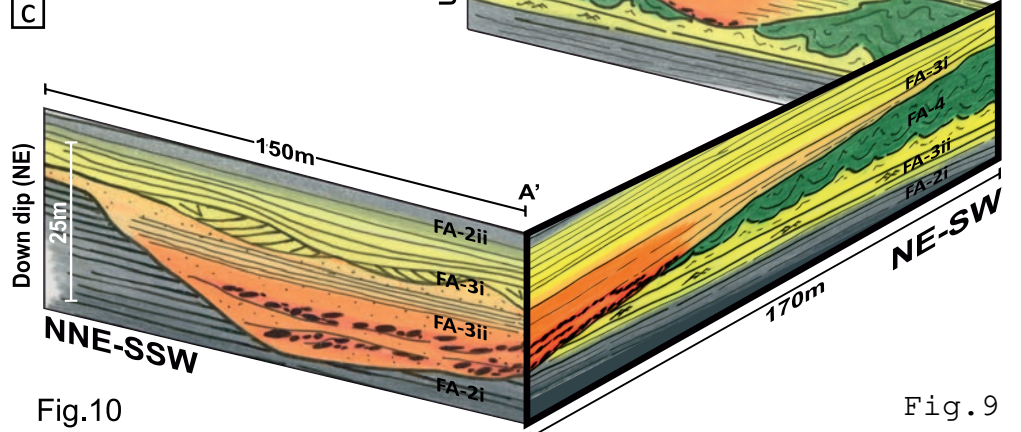
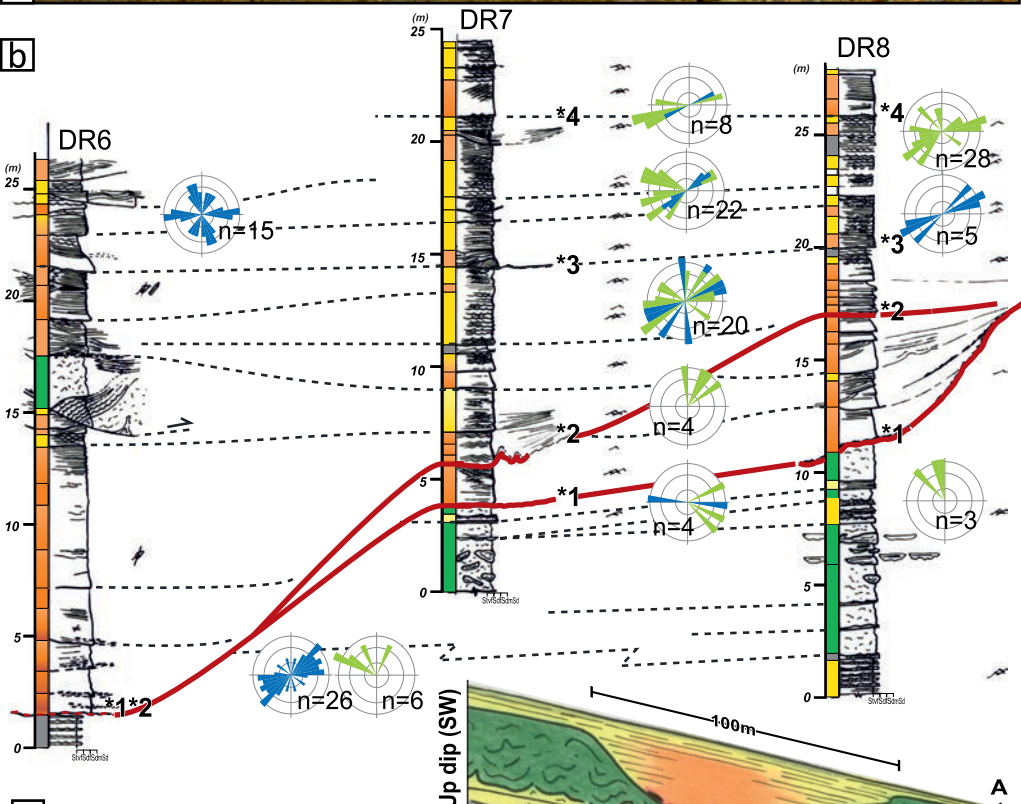
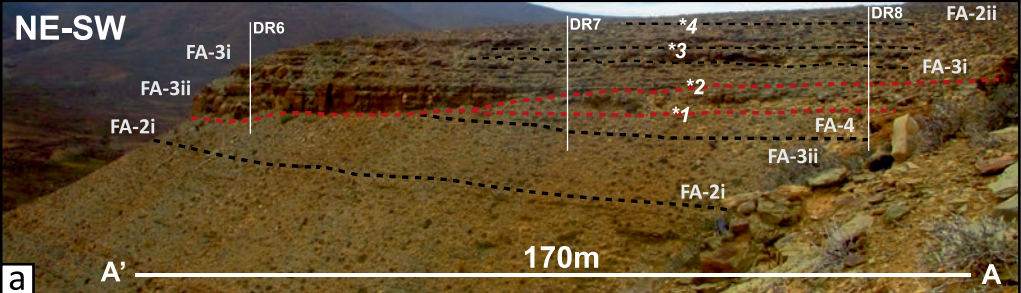


Fig.10

Fig.9



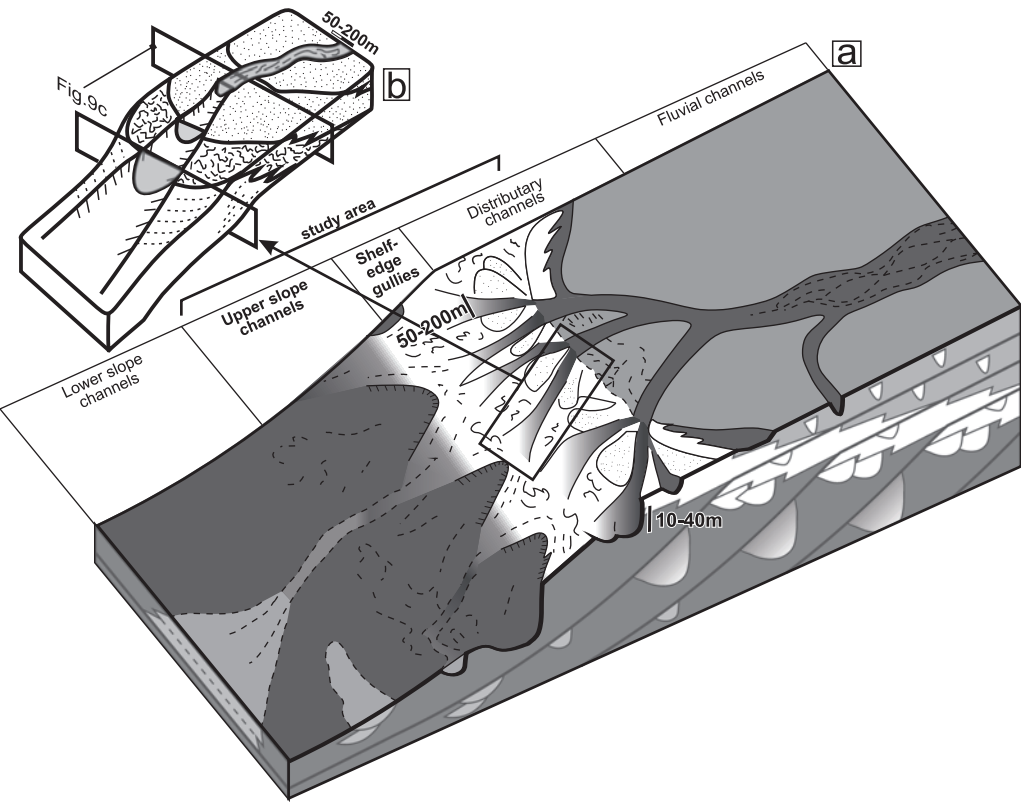


Fig.11

	Lithofacies	Sedimentary structures	Thickness, lithology and textural properties	Process interpretation	Other characteristics	FA
Conglomerate facies (C)	Ci	Matrix- to clast-supported intraformational conglomerate, crudely cross-stratified	cm- to dm- scale, poorly-sorted and matrix- to clast-supported intraformational conglomerate. Siltstone to sandstone matrix, with mudstone, siltstone or sandstone clasts, 0.5-20 cm in diameter. Irregular contacts, commonly erosive bases, poorly formed cross-bedding and gradational tops (Fig.5a).	Locally sourced lithic clasts transported as bedload and deposited as basal lag when flow loses energy. Cross-bedding indicates migration of dunes and bars. Outsize clast content suggests bank collapse and erosion during high energy flows, or channel lateral migration.	Reddening of lags may represent oxidation of iron-rich minerals.	FA-3ii
	Cm	Mudstone clast horizon	Horizons of claystone and siltstone rip-up clasts within fine- or medium-grained sandstone beds. Clasts are up to 20 cm in size, rounded to angular and typically poorly-sorted. Beds are irregular in thickness and often erosional (Fig.5b).	Mudstone clasts entrained from erosion of underlying claystone and siltstone material during scour. Where mudstone clast horizons occur amongst sandstones, this is interpreted as high magnitude, low frequency flows, mobilising the mudstone clasts.	Mud clasts are commonly aligned or imbricated.	FA-3ii
Sandstone facies (S)	Ss	Structureless	cm- to m-scale poorly to moderately-sorted very fine to medium-grained sandstone. Sharp base and top, rarely erosive. Few gradational tops (Fig.5c).	<i>En masse</i> deposition from high velocity and density sediment gravity flows. Uniform narrow grain size range suggests rapid deposition under upper flow regime conditions also suppressing bedform development.	Internal structures overprinted by intensive bioturbation or dewatering. Locally abundant in plant remains and oxidized organic matter.	FA-2, FA-3, FA-4
	Sg	Inverse or normal grading	cm- to m-scale moderately to well-sorted very fine to fine, or medium-grained sandstone. Base and top can be either sharp or gradational (Fig.5d).	Normal grading interpreted to reflect evidence of waning flow conditions. Inverse grading reflects waxing flow conditions attributed to river floods.	Plant debris and mica, and development of composite reverse-graded to graded beds.	FA-2, FA-3, FA-4
	Sp	Parallel bedding	cm- to m-scale moderately to well-sorted very fine to fine-grained sandstone. Sharp top and base, rarely erosive or gradational. Parting lineations are common (Fig.5e).	Deposition under upper phase plane bed conditions. Parting lineations can be produced by turbulent eddies or microvortices at the bed boundary layer. Also interpreted as representing vertical aggradation under shallow flow conditions.	Parting lineation, mud clasts, oxidized organic matter and plant fragments observed in parallel laminae	FA-2, FA-3, FA-4
	Sl	Low angle cross-bedding, SCS or HCS	cm- to m-scale well sorted very fine to fine-grained sandstone. Sharp base and top, rarely erosive. Commonly features undulatory bed tops.	Deposited under low flow regime conditions within large-scale dunes and barforms. Interpreted as representing deposition in broad bedload sheets, during migration downstream, and affected by combined or oscillatory flows.	Well-sorted rounded grains, mud clasts associated to erosive bases and common symmetrical-rippled tops.	FA-2, FA-3, FA-4
	Sx	High angle planar or trough cross-bedding	cm- to m-scale moderately-sorted very fine to medium-grained sandstone. Sharp base and top, rarely erosive. Few gradational tops (Fig.5f).	Planar cross-stratification represents migration of 2-D subaqueous dunes interpreted to represent deposition within deeper and/or faster parts of a confined/channelized flow. Trough cross bedding is interpreted to reflect migration of 3-D dunes through bedload transportation. 3-D dunes occur under lower flow regime conditions, where deeper scours are most prevalent, and are associated with both downstream and laterally accreting barforms.	Mud clasts, oxidized organic matter and plant fragments are observed in cross-sets.	FA-3, FA-4
	Sr	Ripple or climbing ripple-lamination	mm- to dm-scale moderately-sorted very fine to fine-grained sandstone. Generally sharp or gradational bases and asymmetrical rippled tops (Fig.5g).	Tractional bedforms developed under lower flow regime conditions. Asymmetrical current ripples produced by uni-directional flows. Climbing ripples reflecting higher sedimentation rates.	Ripples locally show stoss and lee side preservation.	FA-2, FA-3, FA-4
Mudstone facies (M)	Sw	Wavy lamination and symmetrical ripple-lamination	mm- to dm-scale well-sorted very fine to fine-grained sandstone. Generally sharp or gradational bases and symmetrical rippled tops (Fig.5h).	Tractional bedforms developed under lower flow regime conditions, with symmetrical crests created by bi-directional currents under orbital wave motion. Secondary ladder-back ripple sets formed between larger ripple troughs.	Well-sorted, rounded grains. Common superimposition of interference ripples.	FA-2, FA-3, FA-4
	Ms	Parallel to ripple-laminated, normally and inversely-graded fissile siltstones and mudstones	mm- to dm-scale poorly to moderately-sorted coarse siltstone beds. Contacts are generally gradational. Locally sharp based.	Deposition from very low-density turbidity/hyperpycnal currents, sometimes associated with river floods or storms. Post depositional compaction masks primary sedimentary structures.	Common appearance of starved and lenticular unidirectional ripples.	FA-1, FA-2, FA-4
	Md	Dark grey to black structureless siltstones and mudstones	mm- to m-scale moderately to well-sorted medium to fine siltstone beds. Generally gradational contacts, locally sharp.	Hemipelagic fall-out from low current velocities or low suspended sediment concentrations during conditions of low clastic input. Mode of deposition ensures regional coverage of the mudstone deposits in distal settings.	Often associated with sideritic concretionary horizons.	FA-1, FA-2, (FA-4)
	Mo	Light grey to olive green, structureless to well laminated siltstones and mudstone	cm- to m-scale poorly to moderately-sorted coarse to fine siltstone beds. Generally gradational contacts, locally sharp.	Deposition by direct fallout from suspension, or debris-flows leading to a structureless appearance. Green colouration indicates waterlogged environment.	Local development of carbonate-rich nodular levels.	FA-1, (FA-2)

Table.1